Impact of ~~wave-water~~sea level ~~non-linear interactions for the projections of mean and extreme~~changes on future wave conditions along the coasts of western Europe

Alisée A. Chaigneau[1,2], Stéphane Law-Chune[2], Angélique Melet[2], Aurore Voldoire[1], Guillaume Reffray[2], Lotfi Aouf[3]

[1]CNRM, Université de Toulouse, Météo-France, CNRS, Toulouse, France.
[2]Mercator Ocean International, Toulouse, France.
[3]Météo-France, Toulouse, France.

Correspondence to: Alisée A. Chaigneau (~~achaigneau@mercator-ocean.fr~~alisee.chaigneau@gmail.com)

Abstract. Wind-waves and ~~swell~~swells are ~~a main driver~~major drivers of coastal environment changes~~. Wave setup contributes to~~ and coastal hazards such as coastal flooding ~~during extreme water level events.~~and erosion. Wave characteristics ~~used to estimate wave setup~~ are sensitive to changes in water depth in shallow and intermediate waters. However, wave models used for historical simulations and projections typically do not account for ~~water~~sea level changes whether from tides, storm surges, or long-term sea level rise. In this study, the sensitivity of projected changes in wave characteristics to the non-linear ~~interactions between waves and water~~interaction of sea level ~~changes~~on waves is investigated along the Atlantic European coastline. For this purpose, a global wave model is dynamically downscaled over the northeastern Atlantic for the ~~1950~~1970-2100 period ~~and for two~~under the SSP5-8.5 climate change ~~scenarios (SSP1-2.6 and SSP5-8.5).~~scenario. Twin experiments are performed ~~by accounting (with~~ or ~~not) for~~ without including hourly sea level variations ~~of water level~~ from regional 3D ocean simulations in the regional wave model. The largest ~~impacts~~impact of the non-linear interaction of ~~wave-water~~sea level ~~interactions are found~~on waves is located on the wide continental shelf where shallow water dynamics prevail, especially in macro-tidal areas. For instance, in the Bay of Mont-Saint-Michel in France, due to a ~~large~~ tidal range of 10 m~~. At this location and during an~~, extreme historical ~~extreme event, significant wave height was~~wave heights were found to be up to 1 m higher ~~(or +25~~(+30 %) when ~~considering water~~sea level variations~~.~~ are included. At the end of the 21st century ~~under SSP5-8.5 scenario, the wave simulation including water level variations exhibits an increase in~~, extreme significant wave heights ~~and wave setup values~~are larger by up to +~~20 % and +10 % respectively. These results are found for many coastal points of the large continental shelf where shallow and intermediate water dynamics prevail, and especially so in macro-tidal areas. However, as the wave setup is computed with a parameterization based on offshore characteristics, the depth-induced wave breaking is not activated in the model.~~40 % (+60 cm) mainly due to the effect of tides and mean sea level rise. The estimates provided in this study ~~therefore~~ only partially represent the processes responsible for the ~~wave-water~~sea level-wave non-linear interactions due to model limitations in terms of resolution and processes included.

1 Introduction

Coastal zones are among the most densely populated and urbanized areas in the world (McMichael et al., 2020; Neumann et al., 2015; Wolff et al., 2020)~~.~~, which implies that monitoring their evolution in the context of climate change is important in several aspects. Wind-waves and ~~swell~~swells are ~~a~~ major ~~driver~~drivers of coastal environment changes (Ranasinghe, 2016) and can drive coastal marine hazards such as coastal flooding (Melet et al., 2020b). ~~Coastal marine flooding is most severe during extreme water level events. Extreme water levels actually cause most of the sea level-related damages and are on the rise due to mean sea level rise (e.g. Fox-Kemper et al. 2021, Le Cozannet et al. 2022).~~

~~Wind-waves and swell contribute to extreme water level events at the coast via wave setup and runup, combined with astronomical tides, storm surges (due to low atmospheric surface pressure and wind setup) and mean sea level changes. In this study, wave contribution assessment will be limited to wave setup. Wave setup corresponds to the time-mean (over several wave groups) elevation of the water level in the shallow surf zone due to breaking waves (Dodet et al., 2019; Longuet-Higgins and Stewart, 1964). At a large spatial scale, wave setup usually scales with offshore wave characteristics such as the wave height and wavelength (Holman, 1986; Stockdon et al., 2006; Dodet et al., 2019). As a rule of thumb, wave setup reaches 10-20 % of the significant wave height (Holman, 1986; Guza and Thornton, 1981).~~

To build knowledge on future changes in wave climate, a growing number of global and regional wave projections have been developed and intercompared ~~(Hemer et al., 2013; Hemer and Wand 2017; Morim et al., 2018, 2021; Lobeto et al., 2021; Meucci et al., 2020). Projections are commonly based on dynamical wave models forced by projected surface winds from general circulation models, notably from~~(Hemer et al., 2013; Morim et al., 2018; Meucci et al., 2020; Morim et al., 2021; Lobeto et al., 2021; Morim et al., 2023). These projections are commonly based on dynamical wave models often forced by surface winds projected by climate models contributing to the Coupled Model Intercomparison Project (CMIP), with potential downscaling of atmospheric forcing. ~~Regional dynamic downscaling can be used to provide wave projections at higher~~

resolution. A multi-model analysis is required to assess uncertainties and robustness of projected changes in wave climate changes. Morim et al., 2018, 2019 provided a review of wave projections. Over the northeastern Atlantic and Mediterranean Sea bordering the coasts of western Europe, models project a robust decrease in annual and seasonal mean significant wave height, together with a decrease in the mean wave period. Regarding mean wave direction, a robust clockwise change is projected for the Iberian Atlantic Iberian coast. Extreme significant wave heights are also consistently projected to decrease over the northeastern Atlantic and Mediterranean Sea (Morim et al., 2018, 2021; Aarnes et al., 2017).

Wave characteristics used to estimate wave setup are sensitive to changes in water depth and thus to sea level changesvariations in shallow and intermediate waters, where waves start to interact with the ocean bottom. This occurs through a variety of processes. Very close to the coast, in shallow waters, depth-induced wave breaking is the fundamental mechanism, but it is a very small-scale process comparedthat is often omitted in climate projections due to the coarse resolution of global and regional models used for climate projections.. In intermediate waters, at a greater distance from the coast, other larger scale processes are involved and can also be affected by watersea level variations for instance through bottom friction effects or non-linear interactions between the different waves of the spectrum. However, wave models used for historical simulations and projections typically do not account for water level changes, whether from tides, storm surges, or long-term sea level rise. Yet. At fine spatial scales, wave statistics have already been shown to be sensitive to sea level rise (Chini et al., 2010; Wandres et al., 2017; Arns et al., 2017) and to tide tides and surges during extreme wave events (Alari, 2013; Viitak et al., 2016; Fortunato et al., 2017; Lewis et al., 2019; Staneva et al., 2021; Calvino et al., 2022). A review of tide and sea level rise effects on waves and wave setup is provided in Idier et al., 2019. Tides-wave setup interactions can induce changes in total water level at the coast of a few centimeters to tens of centimeters in some cases (Idier et al., 2019). These studies have mainly been conducted at fine scales including very coastal processes. But on a larger scale and in the context of climate change and sea level rise, projections of wave setup could also differ substantially when non-linear interactions between water level and waves are accounted for, due to other larger scale processes.(Alari, 2013; Viitak et al., 2016; Fortunato et al., 2017; Idier et al., 2019; Lewis et al., 2019; Staneva et al., 2021; Calvino et al., 2022). However, large-scale wave models used for historical simulations and projections typically do not account for sea level changes, whether from tides, storm surges, or long-term sea level rise. Nevertheless, these wave climate simulations are likely to be influenced by sea level variations through small to large scale processes, depending on those included in the model.

The present study aims at investigating the sensitivity of wave mean and extreme characteristicswave climate conditions to the non-linear interactions between waves and waterinteraction of sea level changes. In particular, wave setup is presented as an indicator for coastal hazard related to coastal flooding.on waves. To that aim, regional hindcastshistorical simulations and projections of waves are produced over the 19501970-2100 period considering two climate change scenarios corresponding to low-emissions,the high-mitigation (SSP1-2.6) and high-emissionsemission, low-mitigation (SSP5-8.5) pathwaysclimate change scenario (O'Neill et al., 2016). The simulations are produced over the northeastern Atlantic region, called the IBI domain (Iberian-Biscay-Ireland). The wave model is intended to represent the open ocean wave characteristics therefore the depth-induced wave breaking is not activated. Given that the model resolution is not fine enough to calculate properly the wave setup, it is estimated using a generic parameterization based on offshore characteristics. To assess the sensitivity of wave projectionswaves characteristics to the wave-water level non-linear interactionsinteraction of sea level on waves, the regional wave model is adapted to consider hourly variations of watersea level from a 3D regional ocean model described in Chaigneau et al., 2022 for the same IBI domain..

The paper is organized as follows. GlobalThe wave model and regional wave model configurations and simulations are presented in Sect. 2 together with the calculation of the wave setup contribution. Regional simulations for the northeastern Atlantic domain2. Simulated mean and extreme wave conditions are compared to observations over the historical period and to previously published 21st century projections in Sect. 3, in terms of mean and extreme conditions.. Sect. 4 provides an assessment of the impact of including hourly water level changes on sensitivity of wave characteristics and wave setupto the non-linear interaction of sea level on waves along the European Atlantic coastlines. Finally, results are discussed in Sect. 5 and conclusions are drawn in Sect. 6.

2 Methods: models and simulations

The aim of the present study is to investigate the sensitivity of historical and projected sea states to the wave-water level non-linear interactions for the IBI coastlines. To this end, a regional dynamical downscaling of a global wave model (CNRM-HR-WAV, Sect. 2.3.1) forced by a global climate model (CNRM-CM6-1-HR) was implemented over the northeast Atlantic region. Regional wave simulations (IBI-CCS-WAV, Sect. 2.2) are forced by hourly surface currents from a regionally downscaled ocean model (IBI-CCS, Sect. 2.3.3), using the same CNRM-CM6-1-HR parent climate model. In addition, a twin regional wave configuration was set up to investigate wave-water level interactions by considering hourly water level outputs from IBI-CCS in the wave model (IBI-CCS-WAV_ssh, Sect. 2.4). Figure 1 describes the downscaling strategy and the links between the different models used in this study. All the wave simulations described in the following sections are performed over the historical period (1950-2014) and the 21st century (2015-2100) under the SSP1-2.6 and SSP5-8.5 climate change scenarios.

Mis en forme : Couleur de police : Automatique
Mis en forme : Couleur de police : Automatique
Mis en forme : Couleur de police : Automatique
Mis en forme : Couleur de police : Automatique
Mis en forme : Couleur de police : Automatique
Mis en forme : Couleur de police : Automatique
Mis en forme : Couleur de police : Automatique
Mis en forme : Couleur de police : Automatique
Mis en forme : Couleur de police : Automatique
Mis en forme : Anglais (États-Unis)
Mis en forme : Anglais (États-Unis)
Mis en forme : Anglais (États-Unis)
Mis en forme : Anglais (États-Unis)
Code de champ modifié
Mis en forme : Anglais (États-Unis)
Mis en forme : Couleur de police : Automatique
Mis en forme : Couleur de police : Automatique
Mis en forme : Couleur de police : Automatique
Mis en forme : Couleur de police : Couleur personnalisée(RVB(28;29;30))
Mis en forme : Couleur de police : Couleur personnalisée(RVB(28;29;30))
Mis en forme : Couleur de police : Couleur personnalisée(RVB(28;29;30))
Mis en forme : Couleur de police : Couleur personnalisée(RVB(28;29;30))
Mis en forme : Couleur de police : Automatique
Mis en forme : Couleur de police : Automatique
Mis en forme : Couleur de police : Automatique
Mis en forme : Couleur de police : Automatique
Mis en forme : Couleur de police : Automatique
Mis en forme : Couleur de police : Automatique
Mis en forme : Couleur de police : Automatique
Mis en forme : Couleur de police : Couleur personnalisée(RVB(28;29;30))
Mis en forme : Couleur de police : Automatique
Mis en forme : Couleur de police : Automatique
Mis en forme : Couleur de police : Automatique
Mis en forme : Couleur de police : Automatique
Mis en forme : Couleur de police : Automatique
Mis en forme : Couleur de police : Automatique
Mis en forme : Couleur de police : Automatique
Mis en forme : Couleur de police : Automatique
Mis en forme : Couleur de police : Automatique
Mis en forme : Couleur de police : Automatique
Mis en forme : Couleur de police : Automatique
Mis en forme : Couleur de police : Automatique
Mis en forme : Couleur de police : Automatique
Mis en forme : Couleur de police : Automatique
Mis en forme : Couleur de police : Automatique
Mis en forme : Couleur de police : Noir

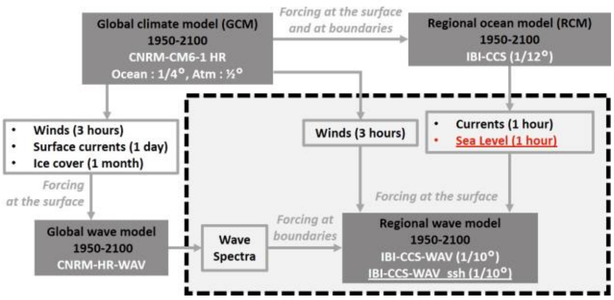

Figure 1: Sketch of the downscaling strategy explaining the links between the different models used in this study.

Two regional wave configurations IBI-CCS-WAV (Sect. 2.2) and IBI-CCS-WAV_ssh (Sect. 2.3) are set up to dynamically downscale global wave simulations over the IBI domain, considering or not hourly sea level outputs as a forcing in the wave model (Sect. 2.1). Table 1 summarizes the different simulations used in the study: the simulations performed and analyzed in this paper, the simulations used for the forcings, the simulations used for the validation in Sect. 3. Appendix A describes the downscaling strategy and the links between the different simulations used to force the regional wave model.

Name of the simulation	Model type	Name of the model	Historical time-span	Future time-span and scenarios	Horizontal resolution	Forcings	Application in the paper	References
IBI-CCS-WAV and IBI-CCS-WAV_ssh	**Regional wave model**	**MFWAM**	**1970-2014**	**2015-2100 (SSP5-8.5)**	**1/10°**	**CNRM-CM6-1-HR (winds) IBI-CCS (surface currents, sea level) CNRM-HR-WAV (wave spectra)**	**Analyses (Sect. 3 and 4)**	-
CNRM-HR-WAV	Global wave model	MFWAM	1970-2014	2015-2100 (SSP5-8.5)	1°	CNRM-CM6-1-HR (winds, surface currents, ice cover)	Forcing	-
IBI-WAV (reanalysis)	Regional wave model	MFWAM	1993-2020	N/A	1/20°	ERA5 (winds), IBIRYS (surface currents) WAVERYS (wave spectra), with assimilated data	Validation (Sect. 3)	Copernicus Marine Service: García San Martín et al., 2021 Toledano et al., 2021
WAVERYS (reanalysis)	Global wave model	MFWAM	1993-2021	N/A	1/5°	ERA5 (winds), GLORYS12V1 (surface currents), with assimilated data	Calibration, Forcing	Law-Chune et al., 2021
CNRM-CM6-1-HR	Global climate model	NEMO3.6 (ocean), APEGE-Climat 6.3 (atm)	1970-2014	2015-2100 (SSP5-8.5)	1/4° ocean ½° atm		Forcing	Voldoire et al., 2019 Saint-Martin et al., 2021
IBI-CCS	Regional ocean model	NEMO3.6	1970-2014	2015-2100 (SSP5-8.5)	1/12°	CNRM-CM6-1-HR	Forcing	Chaigneau et al., 2022
IBIRYS (reanalysis)	Regional ocean model	NEMO3.6	1993-2020	N/A	1/12°	ERA5, GLORYS2V4 ¼° with assimilated data	Forcing	Copernicus Marine Service: Levier et al., 2020

Table 1: List of the different simulations used in the study. The first box is for wave simulations and the second for ocean simulations.

2.1 The numerical wave model: MFWAM

The MFWAM wave model is a spectral sea-state prediction model (wind-wave and swell). It is a modified version of IFS ECWAM-CY41R2 cycle (ECMWF, 2014) developed at Météo-France for their operational applications (Aouf and Lefèvre, 2015). The variables used to force such a model are surface winds, ocean currents and sea ice cover ~~(if relevant for the ocean domain for the latter).~~if relevant for the ocean domain for the latter. Technical details on the model are explained in Law-Chune et al., 2021.

~~MFWAM primarily aims at describing the open ocean sea states. As such, the coastal depth-induced breaking is not activated in the model and overall, the model is not able to resolve very coastal processes such as the shoaling effect even if included. Large-scale processes included in the model are the terms of wave growth by wind, non-linear interactions between waves, dissipation by breaking in deep water referred to as whitecapping, dissipation by friction between long and short waves, bottom friction. These processes, which occur from the deep ocean to intermediate waters, are likely to be affected by the water level variations.~~

~~Additions from Météo-France concern (i) the use and adjustment of the Ardhuin et al., 2010 source term for wave breaking and swell damping dissipation (ST4 physics, Ardhuin et al., 2010), (ii) the use of a Phillips spectrum tail to better constrain the surface roughness for high-frequency waves. The wind input source term is based on Bidlot et al., 2007 and has been improved by considering wave damping by surface friction and sheltering effects for short waves. The non-linear source term uses the discrete interaction approximation (DIA) approach developed by Hasselmann et al., 1985. A better wave propagation around islands, mostly in the Pacific Ocean, is obtained thanks to an island obstructions scheme.~~

MFWAM primarily aims at describing the open ocean sea states. Source terms include physical processes that generate (wave growth by wind), dissipate (white-capping, dissipation by friction between long and short waves, bottom friction and depth-induced wave breaking) or redistribute wave energy (non-linear interactions between waves). The coastal depth-induced breaking that occurs in shallow waters is parametrized using Battjes and Janssen, 1978. All these processes that occur from the deep ocean to the shallow coastal waters are likely to be affected by sea level variations.

Supported by the assimilation of satellite observations, MFWAM is successfully operated within the Copernicus Marine Service (https://marine.copernicus.eu/) to provide near-real time (analyses/forecasts) and multi-year (reanalysis/hindcasts) wave products over both the global ocean and the northeastern Atlantic corresponding to the region of interest in this study.

2.2 Regional wave ~~model: IBI-CCS-WAV~~

~~**Regional wave**~~ **simulations** ~~**IBI-CCS-WAV (IBI Climate Change Scenarios Wave) are produced over the 1950-2100 period using MFWAM (Sect. 2.1) at a 1/10 ° resolution. The configuration was designed over the IBI domain based on a Copernicus Marine Service (CMEMS) configuration (https://doi.org/10.48670/moi-00030). The regional domain covered by IBI-CCS-WAV extends from 27 to 61 ° N and 17 ° W to 8 ° E (Fig. 2), leading to a horizontal resolution ranging from 5.5 to 10 km. IBI-CCS-WAV is used to dynamically downscale the CNRM-HR-WAV global simulations described in Sect. 2.3.1. The dynamical downscaling method allows the resolution of regional processes at a finer scale. The method consists in forcing the regional wave model at its lateral boundaries by wave spectra from the CNRM-HR-WAV larger scale model and at the surface by winds, surface currents and possibly water**~~**without sea level variations** ~~**from simulations performed with other suitable models. The models and simulations that provide these forcings are described in the following sections 2.3 et 2.4. In the regional wave model, the bathymetry used is a smoothed ETOPO1 ocean bathymetry (https://sos.noaa.gov/datasets/etopo1-topography-and-bathymetry/). In our simulations, the wave spectrum is discretized in 24 directions and 30 frequencies starting from 0.035 up to 0.58 Hz. The time step of IBI-CCS-WAV is set to 240 s. Classical integrated wave parameters are generated hourly for IBI-CCS-WAV.**~~**: IBI-CCS-WAV**

The IBI zone is interesting for wave modeling as it contains a variety of physical processes. First, the domain contains strong variations of bathymetry, with a wide continental shelf in the northern part of the domain (North Sea, English Channel) and a ~~tight~~narrow continental shelf in the southern part (Spain, Portugal, Morocco, Mediterranean Sea) (Fig. ~~2~~1). There are also contrasting wave regimes: the Atlantic coasts are subject to very energetic events in terms of significant wave heights, wave periods and energy flows (Masselink et al., 2016; Bruciaferri et al., 2021) whereas the Mediterranean Sea and North Sea are more sheltered areas dominated by wind waves (Chen et al., 2002; Bergsma et al., 2022). In addition, the zone also contains

Mis en forme : Couleur de police : Automatique

Mis en forme : Couleur de police : Automatique

Mis en forme : Couleur de police : Automatique

Mis en forme : Couleur de police : Couleur personnalisée(RVB(17;85;204))

Mis en forme : Couleur de police : Couleur personnalisée(RVB(17;85;204))

Mis en forme : Couleur de police : Couleur personnalisée(RVB(17;85;204))

Mis en forme : Couleur de police : Couleur personnalisée(RVB(17;85;204))

Mis en forme : Couleur de police : Couleur personnalisée(RVB(17;85;204))

Mis en forme : Couleur de police : Couleur personnalisée(RVB(17;85;204))

Mis en forme : Couleur de police : Automatique

Mis en forme : Titre 2, Espace Avant : 0 pt, Après : 0 pt

Mis en forme : Couleur de police : Automatique

Mis en forme : Couleur de police : Automatique

Mis en forme : Couleur de police : Automatique, Anglais (Royaume-Uni)

Mis en forme : Couleur de police : Automatique

Mis en forme : Couleur de police : Couleur personnalisée(RVB(28;29;30))

Mis en forme : Couleur de police : Couleur personnalisée(RVB(28;29;30))

Mis en forme : Couleur de police : Couleur personnalisée(RVB(28;29;30))

Mis en forme : Couleur de police : Couleur personnalisée(RVB(28;29;30))

Mis en forme : Couleur de police : Couleur personnalisée(RVB(28;29;30))

Mis en forme : Couleur de police : Couleur personnalisée(RVB(28;29;30))

Mis en forme : Couleur de police : Couleur personnalisée(RVB(28;29;30)) very different tidal regimes with both macro and micro tidal regimes respectively in the English Channel/Celtic Sea (Valiente et al., 2019; Stokes et al., 2021) and in the Mediterranean Sea.

Mis en forme : Couleur de police : Couleur personnalisée(RVB(28;29;30))

Mis en forme : Couleur de police : Couleur personnalisée(RVB(28;29;30))

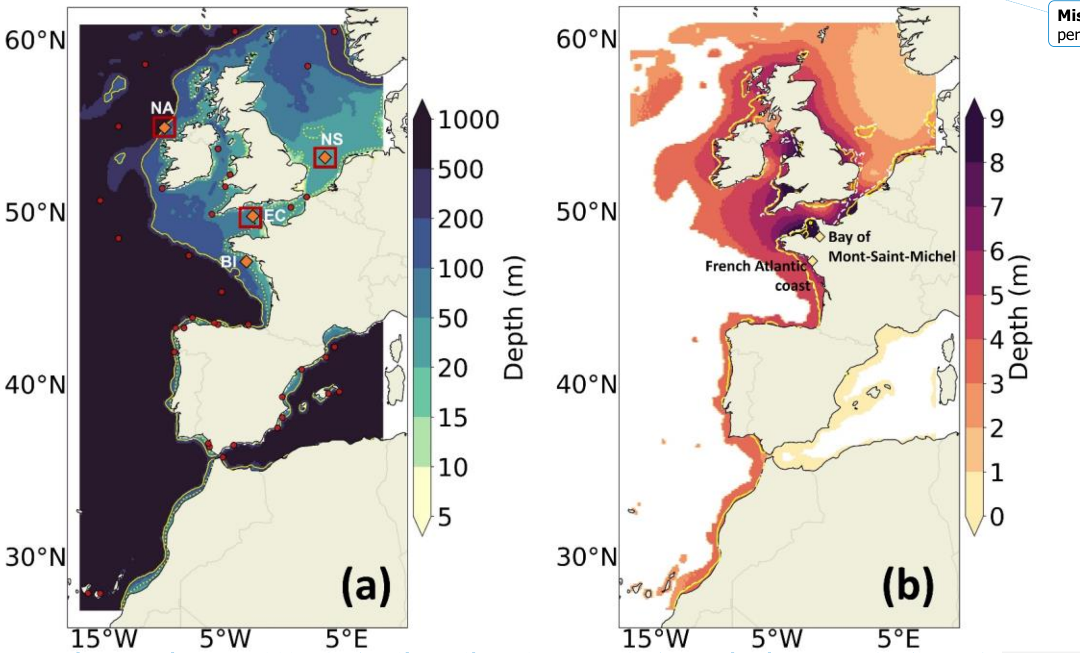

Regional wave simulations IBI-CCS-WAV (IBI Climate Change Scenarios WAVe) are produced using MFWAM (Sect. 2.1) at a 1/10 ° resolution. The configuration was designed over the IBI domain based on the Copernicus Marine Service regional configuration (Tab. 1, IBI-WAV, https://doi.org/10.48670/moi-00030). The regional domain covered by IBI-CCS-WAV extends from 27 to 61 ° N and 17 ° W to 8 ° E (Fig. 1), leading to a horizontal resolution ranging from 5.5 to 10 km. The regional wave configuration is used to dynamically downscale global wave simulations. The dynamical downscaling method allows the resolution of regional processes at a finer scale. The method consists in forcing the regional wave model at its lateral boundaries by wave spectra from the larger scale wave model and at the surface by winds and surface currents from other suitable models (global climate model and 3D regional ocean model, Tab. 1). The models and simulations that provide these forcings are described in the Appendix A. The bathymetry used is a smoothed ETOPO1 ocean bathymetry (https://sos.noaa.gov/datasets/etopo1-topography-and-bathymetry/). The wave simulations are performed over the historical period (1970-2014) and the 21st century (2015-2100) under SSP5-8.5 climate change scenario. Classical integrated wave parameters such as the significant wave height H_s and the peak period T_P are generated hourly.

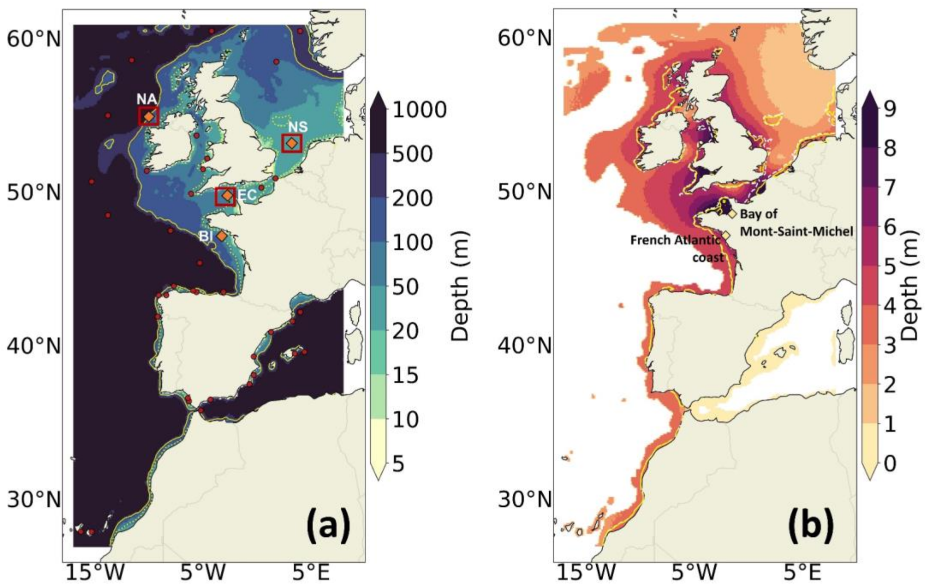

Figure ~~2~~1: (a) Bathymetry (m) of the IBI domain in the regional wave model. The shelf break (defined by the 200 m isobath) is indicated by the solid yellow line. The yellow dotted lines indicate the areas where the waves start to interact with the bathymetry in IBI-CCS-WAV (intermediate waters that cannot be considered as purely deep water), identified when h<L/2 with h the bathymetry and L the mean wavelength over the 1993-2014 period. The red dots represent the locations of the wave buoys from the Copernicus Marine Service (Wehde et al., 2021) used for the validation in Sect. 3.1. The three red boxes are used in ~~Sect. 2.3.2~~Appendix A to validate extreme winds ~~in CNRM-CM6-1-HR.~~of the global climate model. Orange diamonds indicate the wave buoys : used for the wave roses calculation of Sect. 3.1.2 and 3.2.2 (North Atlantic (NA) buoy 6200093 and Belle-Ile (BI) buoy 6200074~~);~~), used for the extreme wind validation ~~of Sect. 4~~in Appendix A (North Atlantic (NA) buoy 6200093, English Channel (EC) buoy 6200103 and North Sea (NS) buoy 6200145). (b) Bathymetric adjustment (Sect. 2.~~4) corresponding here~~3) that corresponds approximately to the M2 tidal range from ~~IBI-CCS~~the 3D regional ocean model (1993-2014). The lines indicate the areas where the waves start to interact with the bathymetry at low tide (dashed white lines) and at high tide (solid yellow lines). The two yellow diamonds indicate the zones where the impact of including hourly ~~water~~sea level outputs in the wave model is assessed in Sect. 4.

2.3 ~~External forcings~~

~~2.3.1 Wave forcing from CNRM-HR-WAV global wave model~~

~~The regional wave model described in Sect. 2.2 is forced at its lateral boundaries by 3-hourly wave spectra information from CNRM-HR-WAV global wave model (Fig. 1). CNRM-HR-WAV simulations are produced over the 1950-2100 period using MFWAM (Sect. 2.1) at a 1 ° resolution. These simulations are forced by 3-hourly surface winds (1/2°), monthly sea-ice cover (1/4 °) and daily ocean surface currents (1/4 °) taken from the CMIP6 CNRM-CM6-1-HR global climate simulations (Voldoire et al., 2019; Saint-Martin et al., 2021). The historical simulation of CNRM-CM6-1-HR is used over the 1950-2014 period. Then, over the 2015-2100 period, the SSP1-2.6 and SSP5-8.5 climate change scenarios simulations are used (O'Neill et al., 2016).~~

~~CNRM-HR-WAV simulations use 2-min gridded global topography data from ETOPO2/NOAA (National Geophysical Data Center 2006). The model grid has a constant spacing in longitude but is compressed in latitude to maintain a constant resolution (Bidlot, 2012). A wave growth calibration was performed to adjust the mean significant wave height of CNRM-HR-WAV to the Copernicus Marine Service WAVERYS wave reanalysis (Law-Chune et al., 2021) over the IBI domain. As for the regional simulations, the wave spectrum is discretized in 24 directions and 30 frequencies starting from 0.035 up to 0.58 Hz. The time step is fixed at 720 s. Classical integrated wave parameters such as significant wave height (Hs) or average wave period (Tm) are generated three-hourly for CNRM-HR-WAV.~~

Mis en forme : Police :10 pt, Couleur de police : Automatique
Mis en forme : Police :10 pt, Couleur de police : Automatique
Mis en forme : Police :10 pt
Mis en forme : Police :10 pt, Couleur de police : Automatique
Mis en forme : Police :10 pt, Couleur de police : Automatique
Mis en forme : Police :10 pt, Couleur de police : Automatique
Mis en forme : Police :10 pt, Couleur de police : Automatique
Mis en forme : Police :10 pt, Couleur de police : Automatique
Mis en forme : Police :10 pt, Couleur de police : Automatique
Mis en forme : Police :10 pt, Couleur de police : Automatique
Mis en forme : Police :10 pt, Couleur de police : Automatique
Mis en forme : Police :10 pt, Couleur de police : Automatique
Mis en forme : Police :10 pt, Couleur de police : Automatique
Mis en forme : Couleur de police : Automatique

2.3.2 Atmospheric forcing from CNRM-CM6-1-HR global climate model

Regional wave projections are driven by the same 3-hourly surface winds as CNRM-HR-WAV (Sect. 2.3.1) produced by the CNRM-CM6-1-HR global climate model (Voldoire et al., 2019; Saint-Martin et al., 2021), which is part of the CMIP6 database. The use of a global climate model with a higher spatial resolution compared to the typical coarse resolutions of CMIP5 and 6 models was interesting for the atmosphere (1/2 °) for the intensity of the winds notably.

By driving our simulations with only one global climate model simulation, the aim of the study is not to characterize the uncertainties of wave projected changes over the IBI domain, but rather to discuss the impact of the water level changes on the downscaled projections. However, before using the winds to force the global and regional wave models, we verified that CNRM-CM6-1-HR was consistent with other CMIP6 global climate models in particular in terms of extreme winds and their projections. A comparison of extreme winds (99th percentile) between CNRM-CM6-1-HR, some other CMIP6 global climate models, the atmospheric reanalysis ERA5 (Hersbach et al., 2020) and wind observations from wave buoys (Wehde et al., 2021) is performed at different locations in the IBI region (Fig. 3a). The three different locations considered (shown in Fig. 2) are chosen along storm trajectories in the northeastern Atlantic and North Sea (Lozano et al., 2004). Figure 3a shows that CNRM-CM6-1-HR is representative of an ensemble of 21 CMIP6 models over the historical period. In general, CNRM-CM6-1-HR is also in good agreement with ERA5 which is the reference here. However, wave buoys observations seem to be significantly different from both the global climate models and ERA5, except in the North Sea. Figure 3b shows the projected changes for the extreme wind speed at the three locations. Projected changes in extreme wind speed are quite small in all models and rather uncertain (large interquartile range). Projected changes are of the same sign for 7, 9 and 10 models out of twelve for the three boxes respectively. In the English Channel and North Sea, CNRM-CM6-1-HR shows an increase in extreme wind speed which is representative of the other CMIP6 models. In the North Atlantic, CNRM-CM6-1-HR exhibits a large decrease in extreme wind speed which is in the high range (in absolute value) of CMIP6 models but still of the same sign as most models.

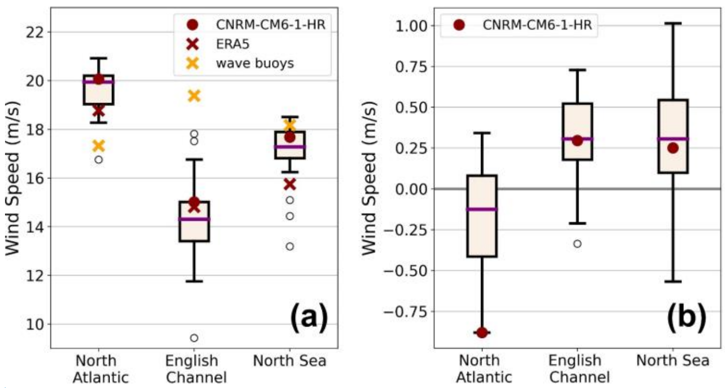

Figure 3: (a) Extreme winds (99th percentile) for CNRM-CM6-1-HR (dark red dot), 21 different CMIP6 global climate models (black box), the atmospheric reanalysis ERA5 (dark red cross) and wind observations from wave buoys (yellow cross) at the three locations in the IBI region marked on Fig. 2a for the 1993-2014 period. The 2011-2022 period was chosen for the wave buoy in the North Sea as it was the only period available. (b) Projected changes in extreme wind speed for CNRM-CM6-1-HR and 12 different CMIP6 climate models at the three locations marked on Fig. 2a under the SSP5-8.5 scenario (2081-2100 vs 1986-2005). The selected CMIP6 climate models are those with three-hourly atmospheric outputs. In (a) and (b), the purple line represents the median, the black box represents the interquartile range and the whiskers represent the last model under or above 1.5 times the interquartile range. The black circles represent the outlier models i.e. models outside 1.5 times the interquartile range. Units are in m s^{-1}.

2.3.3 Ocean forcing from IBI-CCS regional ocean model

Regional wave projections are also forced by the hourly surface current (and hourly water simulations with sea level variations in the dedicated simulation: IBI-CCS-WAV_ssh) of IBI-CCS, a regional ocean model at a 1/12 ° horizontal resolution, itself forced by CNRM-CM6-1-HR global climate model. IBI-CCS was implemented in Chaigneau et al., 2022 to refine sea level projections of CNRM-CM6-1-HR over the northeastern Atlantic region through a dynamical downscaling. For a more complete representation of processes driving coastal water level changes, tides and

Mis en forme : Couleur de police : Automatique, Anglais (États-Unis)
Mis en forme : Couleur de police : Automatique
Mis en forme : Couleur de police : Automatique
Mis en forme : Couleur de police : Bleu
Mis en forme : Couleur de police : Automatique
Mis en forme : Couleur de police : Automatique
Mis en forme : Couleur de police : Automatique
Mis en forme : Couleur de police : Automatique
Mis en forme : Couleur de police : Automatique
Mis en forme : Couleur de police : Automatique
Mis en forme : Police :10 pt, Couleur de police : Automatique
Mis en forme : Police :10 pt, Couleur de police : Automatique
Mis en forme : Police :10 pt, Couleur de police : Couleur personnalisée(RVB(32;33;36))
Mis en forme : Police :10 pt, Couleur de police : Automatique
Mis en forme : Police :10 pt, Couleur de police : Couleur personnalisée(RVB(32;33;36))
Mis en forme : Police :10 pt, Couleur de police : Automatique
Mis en forme : Couleur de police : Automatique
Mis en forme : Titre 2, Espace Avant : 0 pt, Après : 0 pt
Mis en forme : Couleur de police : Automatique
Mis en forme : Couleur de police : Automatique

~~**atmospheric surface pressure forcing are explicitly resolved in IBI-CCS in addition to the ocean general circulation (dynamic sea level).**~~

~~**2.4 Inclusion of water level variations in the regional wave model: IBI-CCS-WAV_ssh**~~

~~The water levels over which the waves propagate control the intermediate and shallow water wave dynamics and the refraction by bathymetric gradients, as well as bottom friction induced wave breaking.~~ To measure the impact of ~~wave-water level~~ the non-linear ~~interactions~~interaction of sea level on waves in the IBI region, a twin configuration to IBI-CCS-WAV (Sect. 2.2) was set up to consider ~~water~~sea level variations as an additional forcing: IBI-CCS-WAV_ssh. For this purpose, MFWAM (Sect. 2.1) has been modified to include ~~an~~ hourly ~~water~~sea level forcing ~~(~~coming from ~~IBI-CCS~~the same 3D regional ocean simulations~~, Sect. 2.3.3) which adjusts bathymetric depth (Fig. 2b) to hydrodynamic effects such~~ as the surface currents. Hourly sea level forcing includes tides, storm surges, mean sea level but also the non-linear interactions between these processes. In our ocean simulations, the mean sea level contains the sterodynamic sea level (thermal expansion and dynamic sea level associated with ocean circulations ~~but also~~) and the barystatic sea level change (the addition of water mass to the ocean); thus, long-term ~~mean~~ sea level rise over the next century~~. In practice, water elevation is read at the same time as ocean surface currents (Fig. 1) and~~ is included in the hourly sea level forcing. From a practical point of view, in order to simulate the sea level variations in the wave model, the sea level obtained from the ocean simulations is added to the ~~topographic depth at each forcing time step. These depth variations associated with water level variations affect the source terms (Sect. 2.1) and wave propagation from intermediate to shallow waters. Wave~~local depth every hour and at every grid point.

The wave model operates with a look-up table system as the following: as a pre-processing, wave propagation parameters such as group velocities and wave numbers, as well as parameters that affect the source terms described in Sect. 2.1 are tabulated ~~at the beginning of the simulation~~ according to a fixed list of depths and frequencies ~~in the form of look-up~~. During the simulation, the required parameters are retrieved from these tables. As explained in Figure 2, the inclusion of sea level affects the local water depth and therefore affects the parameters needed for wave propagation and source terms (Sect. 2.1) in intermediate to shallow waters. The depth discretization ~~for the propagative aspects was adapted~~of the tables follows a geometric series, with a first level at 3 meters and a vertical resolution of ~~the order of~~about 15 centimeters near the surface~~.~~ (Fig. 2). For IBI-CCS-WAV, a minimum water depth of 6 meters was chosen to be consistent with that applied in the forcing from the regional ocean simulations. In the regional ocean model, this value avoids the occurrence of uncovered banks in macro-tidal areas, especially around Mont-Saint-Michel in France and in the Bristol Channel. For IBI-CCS-WAV, since the depth is set to a minimum of 6 meters (Sect. 2.2), values less than 6 meters in the tables are not used. For IBI-CCS-WAV_ssh, since the local depth fluctuates around that of IBI-CCS-WAV, values less than 6 meters in the tables are used, for example at low tide. In this case, the values can be used up to a minimum of 3 meters which corresponds to the first term of the geometric series used to discretize the tables (Fig. 2).

~~A minimum time-mean water depth of 6 meters was chosen to be consistent with that applied in the ocean simulation from IBI-CCS (Chaigneau et al., 2022). This value avoids the occurrence of uncovered banks in macro-tidal areas, especially around Mont-Saint-Michel in France and in the Bristol Channel. These settings are applied for all regional wave simulations, whether they are forced by time-varying water levels (IBI-CCS-WAV_ssh) or not (IBI-CCS-WAV).~~

~~**2.5 Wave setup calculation based on a parametrization**~~

~~The present study aims at investigating the sensitivity of projected changes in mean and extreme wave conditions to wave-water level non-linear interactions. In particular, the focus is given on the wave setup which drives coastal sea level hazards such as coastal flooding. Wave setup and runup can be resolved directly from wave-resolving coastal models such as Xbeach (Roelvink et al., 2009), SWASH (Zijlema et al., 2011) or BOSZ (Pinault et al., 2022). Such models require a high resolution of several meters and nearshore profiles as inputs. They cannot yet simulate nearshore morphological changes over long time periods and at large spatial scales due to their limitations to represent cross-shore sediment exchanges (Elsayed and Oumeraci, 2017). For models such as MFWAM that do not directly resolve the wave setup and runup, they can be estimated, at first order, via empirical formulations that relate them to a set of simple deep water environmental parameters (e.g. Dodet et al., 2019). In our study, the wave contribution to sea level is limited to wave setup. As the aim is to provide a first order estimate of wave setup projected changes, our wave setup estimates η are based on an empirical formulation (Stockdon et al., 2006), applicable for sandy beaches :~~

$$\eta = 0.35\beta\sqrt{H_s L_p} \quad (1)$$ ~~(Stockdon et al., 2006)~~

~~where β is the foreshore beach slope (i.e. the slope in the swash zone), H_s is the deep water significant wave height, L_p is the deep water peak wave wavelength related to the deep water peak wave period T_p through the deep water linear dispersion relationship: $L_p = \frac{g}{2\pi} T_p^{\,2}$, g is the acceleration of gravity.~~

~~As the wave setup estimation largely depends on the beach slope parameter, in this study, for the wave setup changes of Sect. 3.2 and 4, we provided a wave setup scaling $\sqrt{H_s L_p}$ rather than using the formulation of equation (1) to allow our results to be scaled with different beach slopes or empirical formulae (Dodet et al., 2019). To provide a range of wave setup changes~~

Mis en forme : Couleur de police : Automatique

Mis en forme : Non Surlignage

Mis en forme : Non Surlignage

~~estimates, formulation (1) was used with time and space constant beach slope values of 0.04 (4 %) and 0.07 (7 %), which correspond to the low and high spatial-mean values found in previous broad-scale studies (Melet et al., 2020a, Vos et al., 2020). The limitations of such an approach based on parametrizations are discussed in Section 5.~~

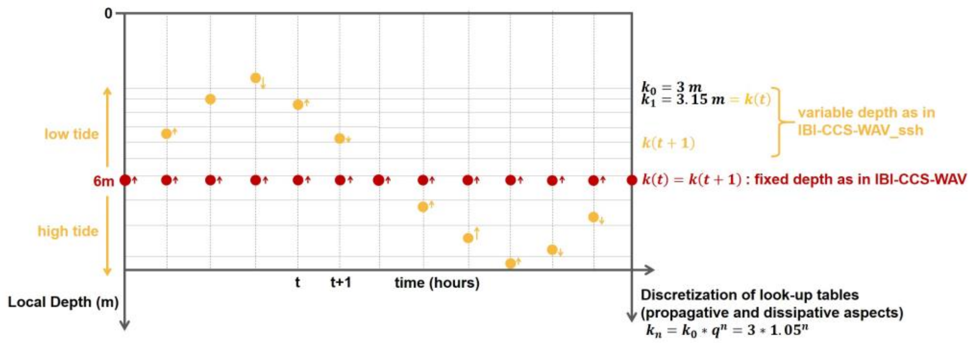

Figure 2: Schematic of the inclusion of sea level variations in the wave model for a given coastal point as a function of time. The dots represent the local depths. In red, the local depth is fixed (IBI-CCS-WAV), and in this example the local depth is the minimum allowed. In yellow, an example of the time evolution of the local depth corresponding to the hourly sea level variations (IBI-CCS-WAV_ssh), here dominated by a tidal signal. The q_n terms represent the vertical discretization of the depths used in the look-up tables to obtain parameters needed for wave propagation and source terms. These discretized depths are chosen as close as possible to the local depths estimated from the bathymetry with sea level changes added.

2.4 Extreme value analyses

To assess the impact of the non-linear interaction of sea level on wave extremes, nonstationary extreme value analyses (EVA) are performed for each coastal location. To do that, the approach of Mentaschi et al., 2016 is used, allowing the detection of long-term trends in extremes and, in our case, the filtering of variability on time scales shorter than 20 years. For each coastal location and wave time series, the output of the EVA is a time-varying generalized Pareto distribution (GPD), from which the return levels can be obtained, such as the 1-in-100-year return level analyzed in Sect. 4.

3 Validation and projections of ~~IBI-CCS-WAV, without waves-sea level interactions~~the regional wave simulations

3.1 Validation of IBI-CCS-WAV and IBI-CCS-WAV_ssh over the 1993-2014 period

IBI-CCS-WAV ~~is~~and IBI-CCS-WAV_ssh are validated over the 1993-2014 period against Copernicus Marine Service products: a regional wave reanalysis ~~which will be referred to as IBI-WAV thereafter (~~(Tab. 1, García San Martín et al., 2021; Toledano et al., 2021) and observations from wave buoys (Wehde et al., 2021). ~~The IBI-WAV reanalysis covers the whole 1993-2020 period and has a horizontal resolution of 5 km. IBI-WAV uses the currents from the IBIRYS regional ocean reanalysis (Levier et al., 2020). In the present~~In this study, we considered the ~~IBI-WAV~~ reanalysis as the reference for the domain ~~as Toledano et al., 2021 have shown that its~~ because it showed good performance ~~was good~~ compared to satellite and buoy observations over the 1993-2019 period~~. The selected wave buoys have a temporal data coverage of at least 60% over the validation period. The 1993-~~ (Toledano et al., 2021). In our case, the 1993-2014 period was chosen for the validation ~~period~~ because it corresponds to the intersection between the period covered by the ~~IBI-WAV~~ regional reanalysis (starting in 1993) and the historical period of IBI-CCS-WAV (ending in 2014).

Wave buoys were selected to have a temporal data coverage of at least 60% over the validation period. The ability of IBI-CCS-WAV and IBI-CCS-WAV_ssh to reproduce observed distributions is assessed for the mean state and the 99th percentile ~~of the~~ significant wave height H_S and peak period ~~since these variables are then used to compute~~T_P and for the mean wave direction through wave roses. In this section, it is rather IBI-CCS-WAV which is validated against the ~~wave setup scaling (Sect. 3.2, 4).~~reanalysis because as IBI-CCS-WAV, the reanalysis does not consider hourly sea level variations as a forcing.

3.1.1 Significant wave height and ~~mean wave~~peak period

Mean state validation

Mis en forme : Couleur de police : Noir
Mis en forme : Couleur de police : Noir
Mis en forme : Couleur de police : Automatique
Mis en forme : Couleur de police : Automatique
Mis en forme : Couleur de police : Automatique
Mis en forme : Couleur de police : Automatique
Mis en forme : Couleur de police : Automatique
Mis en forme : Couleur de police : Automatique
Mis en forme : Couleur de police : Automatique
Mis en forme : Couleur de police : Automatique
Mis en forme : Couleur de police : Automatique
Mis en forme : Couleur de police : Automatique
Mis en forme : Couleur de police : Automatique
Mis en forme : Couleur de police : Automatique, Non Surlignage
Mis en forme : Couleur de police : Automatique
Mis en forme : Couleur de police : Automatique
Mis en forme : Couleur de police : Automatique
Mis en forme : Anglais (Royaume-Uni)
Mis en forme : Couleur de police : Automatique
Mis en forme : Couleur de police : Automatique

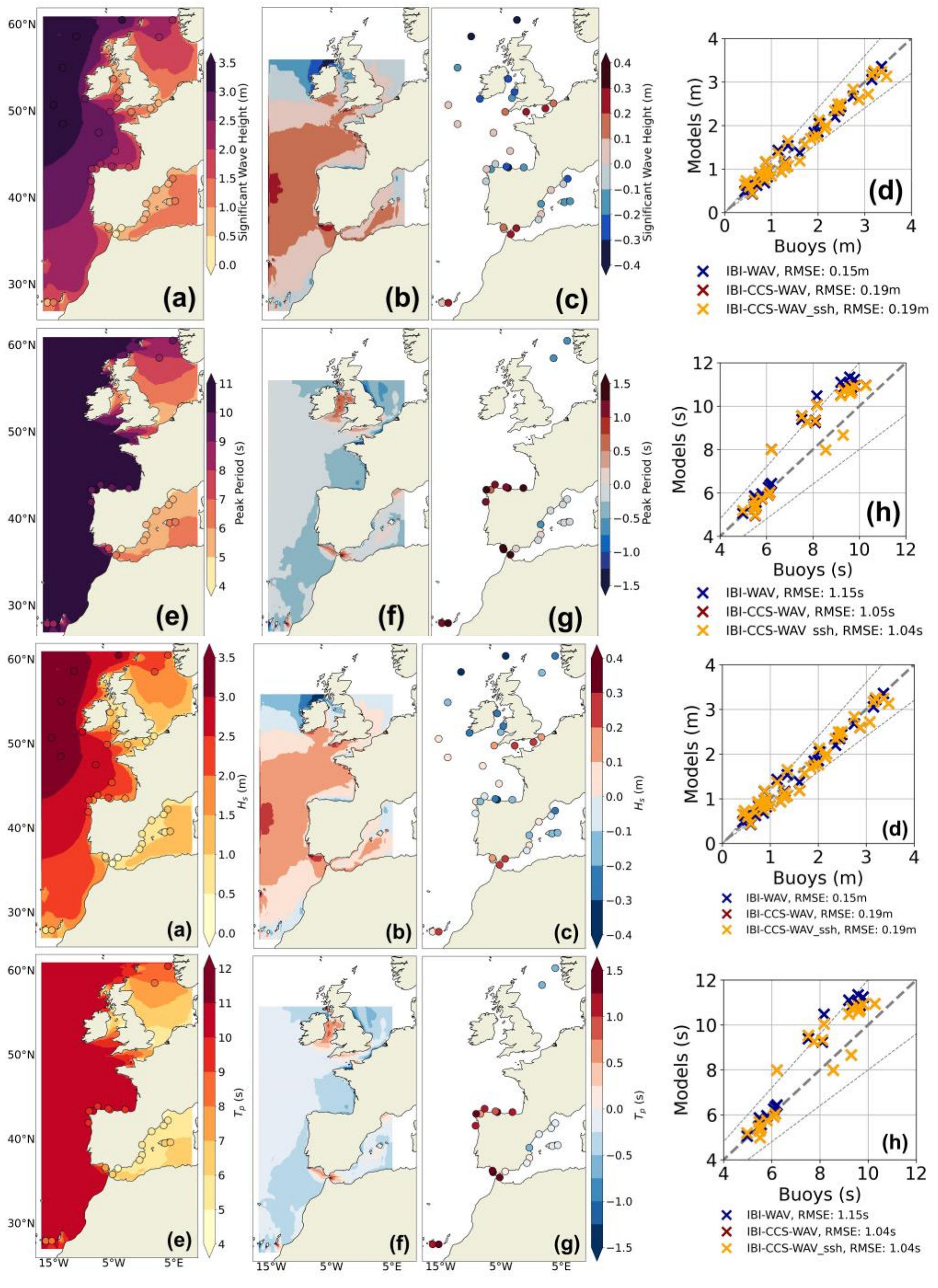

Figure ~~4~~3: (a), (b), (c) and (d) show the mean significant wave height (~~Hs,~~H_s, in m) over the 1993-2014 period for: (a) IBI-CCS-WAV~~.~~ for the domain and wave buoys for the circles. (b) Differences between IBI-CCS-WAV and the reanalysis ~~IBI-WAV~~. (c) Bias between IBI-CCS-WAV and ~~CMEMS~~ wave buoys at buoys locations. (d) Scatter plot at each wave buoy location of ~~simulations~~ IBI-CCS-WAV (red marks), IBI-CCS-WAV_ssh (yellow marks) and ~~IBI-WAV~~the

Mis en forme : Police :10 pt, Couleur de police : Automatique

Mis en forme : Police :10 pt, Couleur de police : Automatique

Mis en forme : Police :10 pt, Couleur de police : Automatique

Mis en forme : Police :10 pt, Couleur de police : Automatique

Mis en forme : Police :+Corps (Times New Roman), 10 pt, Couleur de police : Automatique

Mis en forme : Police :+Corps (Times New Roman), 10 pt, Couleur de police : Automatique

Mis en forme : Police :+Corps (Times New Roman), 10 pt, Couleur de police : Automatique

Mis en forme : Police :+Corps (Times New Roman), 10 pt, Couleur de police : Automatique

Mis en forme : Police :+Corps (Times New Roman), 10 pt, Couleur de police : Automatique

Mis en forme : Police :+Corps (Times New Roman), 10 pt, Couleur de police : Automatique

reanalysis (blue marks) vs observations. (e), (f), (g) and (h) are the corresponding figures for peak period (~~Tp,~~T_P, in s). ~~Note~~(h) must be interpreted with caution as the ~~different color bars in (a) and (b), (c), and in (e) and (f), (g).~~observations are scarce. For (b) and (f) the domain is limited to the domain distributed by the Copernicus Marine Service, with a cut in the northern part. In (d) and (h), the thin dashed lines indicate the 20 % error margin. The RMSE is calculated as the root mean squared deviations from the line y=x (spatial RMSE).

~~Figure 4 illustrates the mean state validation of the IBI-CCS-WAV simulation against the IBI-WAV reanalysis and observations from wave buoys. In general, the~~The mean significant wave height and mean peak period of IBI-CCS-WAV ~~seem to be~~are validated in Figure 3 and are in reasonable agreement with both the reanalysis ~~IBI-WAV~~ and the wave buoys over the 1993-2014 period. ~~Around 40~~The performance of IBI-CCS-WAV and the reanalysis against wave buoys data is quite similar on average over the domain with a root mean square error (RMSE) of the same order of magnitude: about 20 cm for the mean significant wave height and 1 s for the mean peak period (Fig. 3d,h).

Between 35 °N and 45 °N in the deep ocean, IBI-CCS-WAV nevertheless exhibits a positive bias for the mean significant wave height ~~inherited from~~compared to the ~~global wave model forcing through the boundaries~~reanalysis (Fig. ~~4b~~3b). This feature is due to the ~~wind forcing~~westerlies taken from the ~~CNRM-CM6-1-HR (Sect. 2.3.~~global climate model (Tab. 1~~). In CNRM-CM6-1-HR, the westerlies are slightly~~ and Appendix A) that are shifted southward. As ~~a result,~~such, the significant wave heights used as boundary forcings are slightly overestimated in the ~~IBI-CCS-WAV~~ southern domain and underestimated in the northern ~~part of the~~ domain~~,~~ around Ireland, leading to an overall relative error of 10 %. ~~In~~ Differences in the ~~deep ocean, the peak period~~mean state of ~~IBI-CCS-WAV seems to be in good agreement with the reanalysis IBI-WAV (Fig. 4f). However, the~~ significant wave height and peak period ~~differences~~ between IBI-CCS-WAV and ~~IBI-WAV~~the reanalysis are often larger in coastal zones and can reach a relative error of 20 % in the Gulf of Cadiz (Fig. ~~4a,b,e and~~ 3b,f). ~~Differences~~These differences in coastal zones are mainly ~~arise from~~due to the different forcing in the surface currents ~~forcings, coming from IBI-CCS for IBI-CCS-WAV and from IBIRYS (Levier et al., 2020) for IBI-WAV. The currents are~~(Tab. 1), which is particularly different around the Strait of Gibraltar. ~~At this location, the incoming transport and the currents from IBIRYS are more intense than those of IBI-CCS. Indeed, IBI-CCS has been corrected in Chaigneau et al. 2022 to obtain a more accurate transport through the Strait of Gibraltar.~~

~~Figure 4c displays the mean significant wave height biases between IBI-CCS-WAV and wave buoys over the 1993-2014 period. The spatial pattern of the biases is generally in agreement with Figure 4b showing a negative bias in the northern part of the domain and a positive bias~~For the mean peak period, around the ~~Strait of Gibraltar (Fig. 4b and c). Around the~~ Iberian Peninsula, the biases ~~found for the peak period~~ between IBI-CCS-WAV and the reanalysis ~~IBI-WAV~~(Fig. 3f) seem to be in contradiction with those found between IBI-CCS-WAV and the wave buoys (Fig. ~~4f and g~~3g). Toledano et al~~.,~~. 2021 also reported large errors between the reanalysis and wave buoys on the mean wave period in northern Spain ~~between IBI-WAV and the wave buoys for the mean wave period.~~. The uncertainty ~~seems~~appears to be large in this region and IBI-CCS-WAV is within the uncertainty range ~~of uncertainties. The scatter plots of Figure 4d and h show that the performances of both IBI-CCS-WAV and IBI-WAV are quite similar on average over the domain with a root mean square error (RMSE) of the same order of magnitude: about 20 cm for the significant wave height and 1 s for the peak period. Figure 4h must be interpreted with caution as the observations of peak period are scarce and located close to the coast. Most likely coastal buoys are subject to very local effects that are poorly represented at the 1/10 ° model resolution (Fig 4g,h).~~.

~~The comparison of IBI-CCS-WAV_ssh with the reanalysis is not relevant since the latter does not consider the forcing with hourly sea level variations.~~ The IBI-CCS-WAV_ssh simulation is compared to the buoy data in ~~Figure 4d,h and Figure 5,d,h. However, it is difficult to get useful information from these comparisons with~~ the scatter plots (Fig. 3d,h) and Fig. 4d,h) but the performance of IBI-CCS-WAV_ssh is similar to that of IBI-CCS-WAV since the buoys ~~since they~~ are ~~not~~mostly located ~~at the coast. Actually, they are~~ in ~~areas where there is no impact of the wave-water level non-linear interactions~~deep waters (Sect. 4~~) so the performances of IBI-CCS-WAV_ssh are similar to those of IBI-CCS-WAV.~~).

Extreme validation: 99^{th} percentile

Mis en forme : Police :+Corps (Times New Roman), 10 pt, Couleur de police : Automatique
Mis en forme : Police :+Corps (Times New Roman), 10 pt, Couleur de police : Automatique
Mis en forme : Police :+Corps (Times New Roman), 10 pt, Couleur de police : Automatique
Mis en forme : Police :Gras, Couleur de police : Automatique
Mis en forme : Couleur de police : Automatique
Mis en forme : Couleur de police : Couleur personnalisée(RVB(28;29;30))
Mis en forme : Couleur de police : Automatique
Mis en forme : Couleur de police : Automatique
Mis en forme : Couleur de police : Automatique
Mis en forme : Couleur de police : Automatique
Mis en forme : Couleur de police : Automatique
Mis en forme : Couleur de police : Automatique
Mis en forme : Couleur de police : Automatique
Mis en forme : Couleur de police : Automatique
Mis en forme : Couleur de police : Automatique
Mis en forme : Couleur de police : Automatique
Mis en forme : Couleur de police : Automatique
Mis en forme : Couleur de police : Automatique
Mis en forme : Couleur de police : Automatique
Mis en forme : Couleur de police : Automatique
Mis en forme : Couleur de police : Automatique
Mis en forme : Couleur de police : Automatique
Mis en forme : Couleur de police : Automatique
Mis en forme : Couleur de police : Automatique
Mis en forme : Couleur de police : Automatique
Mis en forme : Couleur de police : Automatique
Mis en forme : Couleur de police : Automatique
Mis en forme : Couleur de police : Automatique
Mis en forme : Couleur de police : Automatique
Mis en forme : Couleur de police : Automatique
Mis en forme : Couleur de police : Automatique
Mis en forme : Couleur de police : Automatique
Mis en forme : Non Surlignage
Mis en forme : Non Surlignage
Mis en forme : Couleur de police : Automatique

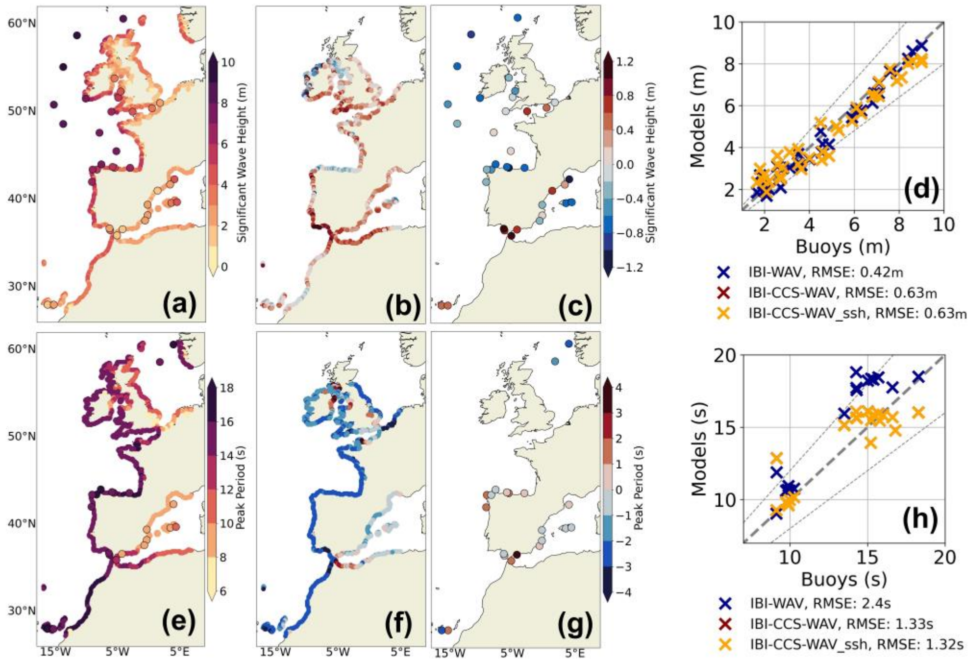

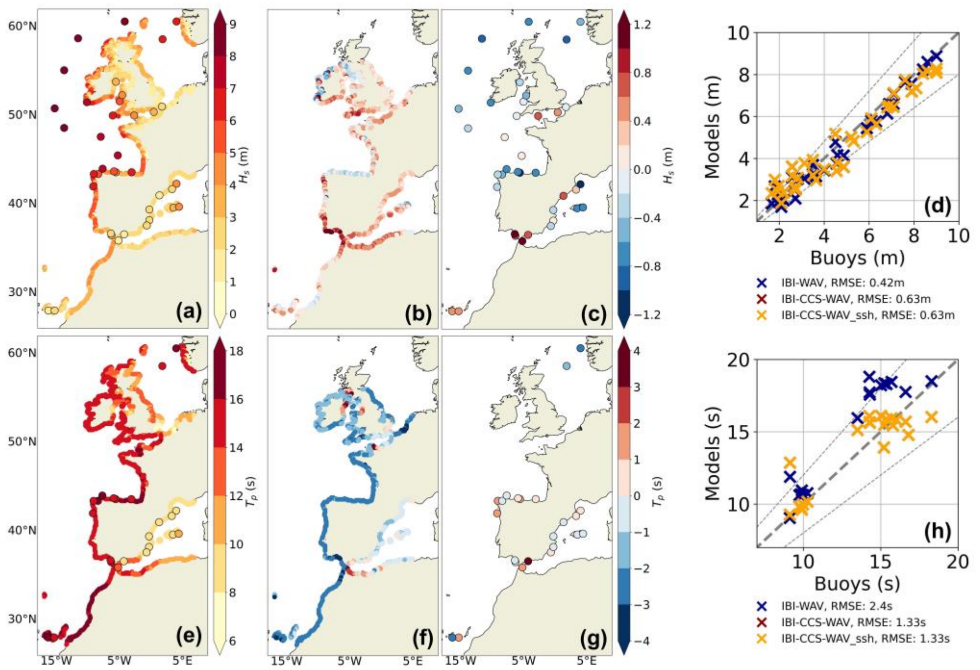

Figure ~~5~~4: (a), (b), (c) and (d) show the 99th percentile (based on hourly outputs) coastal significant wave height (~~Hs,~~H_s in m) over the 1993-2014 period for: (a) IBI-CCS-WAV. for the domain and wave buoys for the circles, (b) Differences between IBI-CCS-WAV and the reanalysis ~~IBI-WAV~~, (c) Bias between IBI-CCS-WAV and ~~CMEMS~~ wave buoys at buoys locations, (d) Scatter plot at each wave buoy location of simulations IBI-CCS-WAV (red marks), IBI-CCS-WAV_ssh

Mis en forme : Police :10 pt, Couleur de police : Automatique

Mis en forme : Police :10 pt, Couleur de police : Automatique

Mis en forme : Police :10 pt, Couleur de police : Automatique

Mis en forme : Police :10 pt, Couleur de police : Automatique

Mis en forme : Police :10 pt, Couleur de police : Automatique

Mis en forme : Police :10 pt, Couleur de police : Automatique

Mis en forme : Police :10 pt, Couleur de police : Automatique

Mis en forme : Police :+Corps (Times New Roman), 10 pt, Couleur de police : Automatique

Mis en forme : Police :10 pt, Couleur de police : Automatique

(yellow marks) and ~~IBI-WAV~~the reanalysis (blue marks) vs observations. (e), (f), (g) and (h) are the corresponding figures for the coastal peak period (~~Tp,~~T_P, in s). (h) must be interpreted with caution as the observations are scarce. Note the different color bars in (a) and (b), (c), and in (e) and (f), (g). For (b) and (f) the domain is limited to the domain distributed by the Copernicus Marine Service, with a cut in the northern part. In (d) and (h), the thin dashed lines indicate the 20% error margin. The RMSE is calculated as the root mean squared deviations from the line y=x (spatial RMSE). Note that the color scales for the biases are larger than for Figure 43.

~~Figure 5 illustrates the validation of extremes (99^{th} percentile) in the IBI-CCS-WAV simulation.~~ The ~~scatter plots of Figure 5d and 5h show that IBI-CCS-WAV satisfactorily reproduces~~ extreme significant wave ~~heights~~height and extreme peak period of IBI-CCS-WAV are validated in Figure 4 and ~~peak periods~~are satisfactorily reproduced by the model, with an overall relative error of 14 % and 9 % for ~~Hs~~ H_s and ~~Tp,~~T_P, respectively~~.~~ (Fig. 4d,h). These values are comparable ~~in value~~ to the relative error of 13 %, 18 % and 20 % found in Lobeto et al., 2021 for the 1-in-5-, 1-in-20- and 1-in-50-year ~~return periods of~~ significant wave ~~height.~~

heights in global wave simulations. The ~~performances~~performance of both IBI-CCS-WAV and ~~IBI-WAV are~~the reanalysis is close, with a slight underestimation of the largest extreme significant wave heights ~~in both models~~. In addition, IBI-CCS-WAV seems to overestimate the smallest 99^{th} percentile of significant wave height, particularly in the Gulf of Cadiz and around the Strait of Gibraltar where the values are 1 m too large (~~Figure 5b and~~ Fig. 4b,c). This feature is also mainly associated with the ~~currents which are quite~~ different ~~around the Strait of Gibraltar~~current forcing in ~~IBI-CCS-WAV compared to those of IBI-WAV due to the complexity of the~~ this very complex zone. ~~Figure 5f shows~~For the ~~comparison of the~~extreme peak ~~period 99^{th} percentile between IBI-WAV and IBI-CCS-WAV. Differences~~periods, differences of 3 s (relative error of 20 %) are found ~~between IBI-CCS-WAV and IBI-WAV~~ along the Atlantic coasts ~~(Fig. 5f~~between IBI-CCS-WAV and the reanalysis (Fig. 4f). However, this feature seems to be related to an overestimation of the extreme peak periods in the reanalysis ~~IBI-WAV~~ as the differences do not appear when IBI-CCS-WAV is ~~directly~~ compared to wave buoys (Fig. ~~5g). The scatter plot of Figure 5h also shows a smaller RMSE with IBI-CCS-WAV than with IBI-WAV when compared to wave buoys.~~4g,h). This overestimation is ~~also~~ reported in Toledano et al., 2021 in which the reanalysis ~~IBI-WAV~~ is validated.

Mis en forme : Police :10 pt, Couleur de police : Automatique
Mis en forme : Police :10 pt, Couleur de police : Automatique
Mis en forme : Police :10 pt, Couleur de police : Automatique
Mis en forme : Police :+Corps (Times New Roman), 10 pt, Couleur de police : Automatique
Mis en forme : Police :10 pt, Couleur de police : Automatique
Mis en forme : Police :10 pt, Couleur de police : Automatique
Mis en forme : Couleur de police : Automatique
Mis en forme : Couleur de police : Automatique
Mis en forme : Couleur de police : Automatique
Mis en forme : Couleur de police : Automatique
Mis en forme : Couleur de police : Automatique
Mis en forme : Couleur de police : Automatique
Mis en forme : Couleur de police : Automatique
Mis en forme : Couleur de police : Automatique
Mis en forme : Couleur de police : Automatique
Mis en forme : Couleur de police : Automatique
Mis en forme : Couleur de police : Automatique
Mis en forme : Couleur de police : Automatique
Mis en forme : Couleur de police : Automatique
Mis en forme : Couleur de police : Automatique
Mis en forme : Couleur de police : Automatique
Mis en forme : Couleur de police : Automatique
Mis en forme : Couleur de police : Automatique
Mis en forme : Couleur de police : Automatique
Mis en forme : Couleur de police : Automatique
Mis en forme : Couleur de police : Automatique
Mis en forme : Couleur de police : Automatique
Mis en forme : Couleur de police : Automatique
Mis en forme : Couleur de police : Automatique
Mis en forme : Couleur de police : Automatique
Mis en forme : Couleur de police : Automatique
Mis en forme : Couleur de police : Automatique
Mis en forme : Couleur de police : Automatique
Mis en forme : Couleur de police : Automatique
Mis en forme : Couleur de police : Automatique
Mis en forme : Couleur de police : Automatique
Mis en forme : Couleur de police : Automatique
Mis en forme : Couleur de police : Automatique

3.1.2 Wave roses

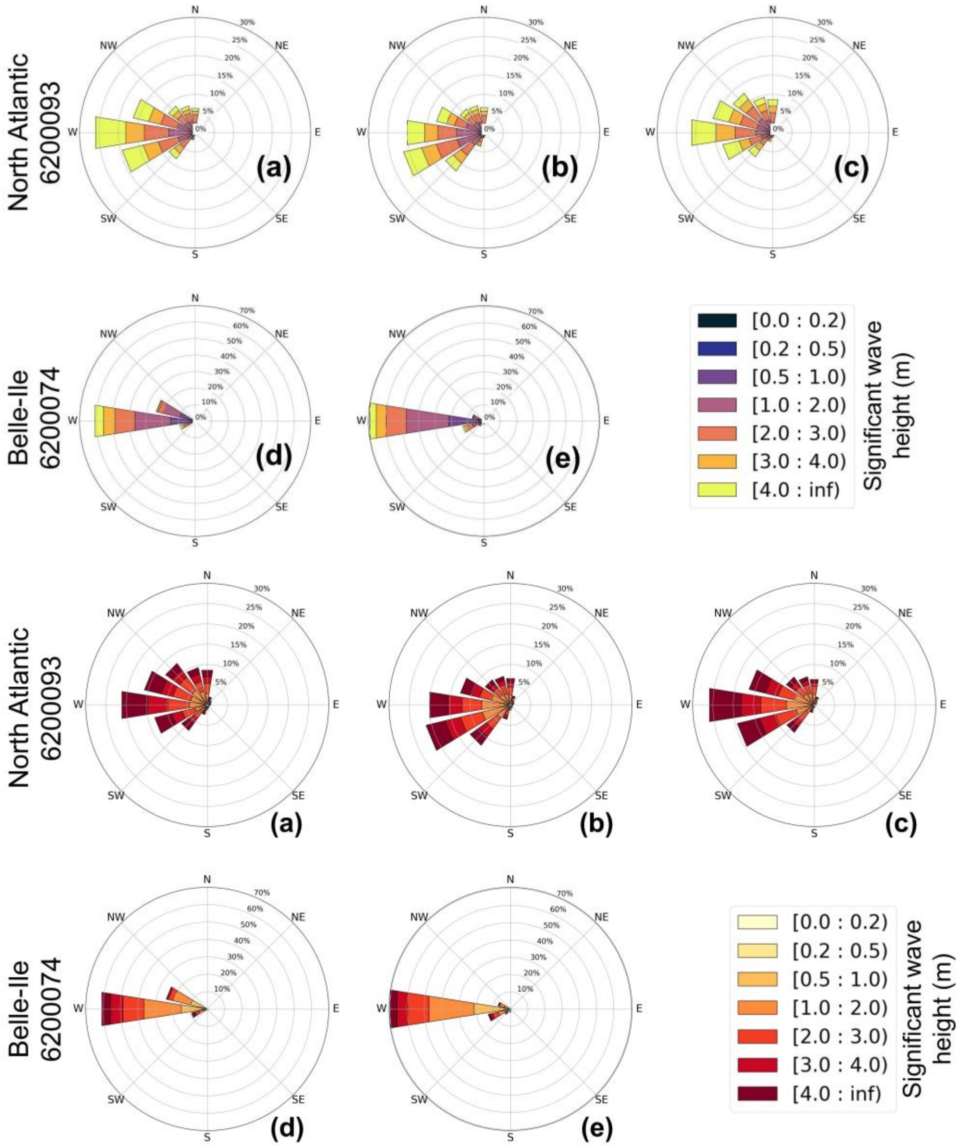

Figure ~~6~~5: Directional distributions of significant wave height at star locations of Fig. ~~2a~~1a: North Atlantic buoy 6200093 (first row), Belle-Ile buoy 6200074 (French Atlantic coast, second row). First column ~~(a,d)~~ are the wave roses based on wave buoy data over the (a) 2003-2022 ~~period for (a)~~ and (d) 2005-2022 ~~for (d).~~periods. Second column (b,e) are the roses for IBI-CCS-WAV over the 1993-2014 period and last column (c) for the ~~IBI-WAV~~ reanalysis over the 1993-2014 period. Different periods are chosen for the wave buoys because of the lack of data for the wave direction over the 1993-2014 period. Wave roses at North Atlantic buoy 6200093 location were computed using mean wave direction. Wave roses at Belle-Ile buoy 6200074 location were computed using the wave direction at spectral peak as it was the data provided by the wave buoy. However, this variable was not an output of the ~~IBI-WAV~~ reanalysis. Colors indicate the wave height distribution in each direction bin.

Mis en forme : Police :10 pt, Couleur de police : Automatique
Mis en forme : Police :10 pt, Couleur de police : Automatique
Mis en forme : Police :10 pt, Couleur de police : Automatique
Mis en forme : Police :10 pt, Couleur de police : Automatique
Mis en forme : Police :10 pt, Couleur de police : Automatique
Mis en forme : Police :10 pt, Couleur de police : Automatique
Mis en forme : Police :10 pt, Couleur de police : Automatique
Mis en forme : Police :10 pt, Couleur de police : Automatique
Mis en forme : Police :10 pt, Couleur de police : Automatique
Mis en forme : Police :10 pt, Couleur de police : Automatique
Mis en forme : Police :10 pt, Couleur de police : Automatique
Mis en forme : Police :10 pt, Couleur de police : Automatique, Anglais (Royaume-Uni)

Directional distributions are ~~shown~~validated on wave roses at two locations in the Atlantic Ocean ~~(~~marked on Fig. ~~2a). In Figure 6, the~~1a (Fig. 5). The focus is only on the IBI-CCS-WAV simulation ~~as we found that the impact of the water level variations on the mean wave direction was negligible over the 1993-2014 period. As both locations~~since the two buoys are ~~found~~located in deep waters (Fig. 1a). Since both sites are located in the Atlantic Ocean exposed to the westerlies ~~exposed Atlantic Ocean~~, the wave roses indicate dominant waves in the west, west-northwest and west-southwest directions. For the North Atlantic buoy 6200093, ~~IBI-WAV shows the same main west direction as~~ both the ~~buoy data (Fig. 6a~~reanalysis and ~~c). However, the observed west distribution is slightly underestimated (by 5 %) by IBI-CCS-WAV and IBI-WAV, especially for the highest waves, superior to 4 m. In IBI-WAV, this could be~~ IBI-CCS-WAV tend to have a southward direction bias compared to the wave buoy associated with a ~~larger~~smaller directional spread of the biggest waves coming from the north (Fig. 5a,b,c). For the reanalysis, ~~6c). In IBI-CCS-WAV, waves tend to have a slight southward direction bias, as~~ the dominant wave direction is west as for the buoy (Fig. 5a,c) while in IBI-CCS-WAV the dominant wave direction is west-southwest (Fig. ~~6b~~5b). For the Belle-Ile buoy 6200074, the west direction represents 70 % of occurrence in IBI-CCS-WAV against 60 % for the wave buoy (Fig. ~~6d~~5d and e). ~~Half of the 70 % are related to~~This difference is coming from waves with a significant wave height of less than 2 m ~~whereas for the buoy it represents only 25 %. This difference of 25 % is~~ found in the west-northwest direction ~~bin~~ for the ~~wave~~ buoy data.

~~Overall,~~In summary, both the IBI-CCS-WAV and IBI-CCS-WAV_ssh regional wave ~~model has shown~~simulations show good ~~performances~~performance compared to the ~~IBI-WAV~~ reanalysis and wave buoys, although observations are scarce. ~~For the future period, as in the present study we use a single global climate model forcing, we assess the regional projections compared to previous published studies.~~

3.2 Regional wave projections of IBI-CCS-WAV under ~~two climate change scenarios:~~ the SSP5-8.5 ~~and SSP1-2.6~~climate change scenario

Regional projections ~~over 2015-2100~~ for the end of the 21st century are now presented for IBI-CCS-WAV under the SSP5-8.5 ~~and SSP1-2.6 scenarios~~climate change scenario for the significant wave height ~~and~~, peak period and mean wave direction validated in Sect. 3.1 ~~and for wave setup scaling $\sqrt{H_s L_p}$ (Sect. 2.5.3).~~

~~3.2.1~~ . By driving our regional simulations with a single global climate model, the aim of the study was not to provide regional wave projections with characterized uncertainties over the domain. Nonetheless, we verified that our regional projections were consistent with other large-scale studies. Projected changes ~~in significant wave height, peak period and wave setup scaling~~for IBI-CCS-WAV_ssh are not presented in this section because they are not directly comparable to other studies that do not include sea level variations, this simulation will be used to characterize the impact of the non-linear interaction of sea level on waves in Sect. 4.

~~**Mean state projections**~~

Mis en forme : Couleur de police : Automatique
Mis en forme : Anglais (Royaume-Uni)
Mis en forme : Anglais (Royaume-Uni)
Mis en forme : Couleur de police : Automatique
Mis en forme : Couleur de police : Automatique
Mis en forme : Couleur de police : Automatique
Mis en forme : Couleur de police : Automatique
Mis en forme : Couleur de police : Automatique
Mis en forme : Couleur de police : Automatique
Mis en forme : Couleur de police : Automatique
Mis en forme : Couleur de police : Automatique
Mis en forme : Couleur de police : Automatique
Mis en forme : Couleur de police : Automatique
Mis en forme : Couleur de police : Automatique
Mis en forme : Couleur de police : Automatique
Mis en forme : Couleur de police : Automatique
Mis en forme : Couleur de police : Automatique
Mis en forme : Couleur de police : Automatique
Mis en forme : Couleur de police : Automatique
Mis en forme : Couleur de police : Automatique
Mis en forme : Couleur de police : Automatique
Mis en forme : Couleur de police : Automatique
Mis en forme : Couleur de police : Automatique
Mis en forme : Couleur de police : Automatique
Mis en forme : Couleur de police : Automatique
Mis en forme : Couleur de police : Automatique
Mis en forme : Couleur de police : Automatique
Mis en forme : Couleur de police : Automatique
Mis en forme : Couleur de police : Automatique
Mis en forme : Normal, Espace Avant : 12 pt, Après : 12 pt, Sans numérotation ni puces
Mis en forme : Couleur de police : Automatique
Mis en forme : Couleur de police : Automatique

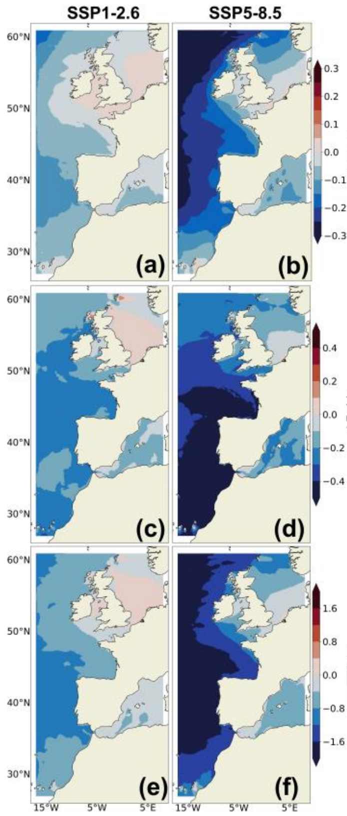

SSP1-2.6
SSP5-8.5
60°N
50°N
40°N
30°N
(a)
(b)
(c)
(d)
(e)
(f)
0.3
0.2
0.1
0.0
−0.1
−0.2
−0.3
Δ Hs (m)
0.4
0.2
0.0
−0.2
−0.4
Δ Tp (s)
1.6
0.8
0.0
−0.8
−1.6
15°W
5°W
5°E

3.2.1 ~~Figure 7:~~ Projected changes in ~~incoming waves~~mean and extreme significant wave height and peak period

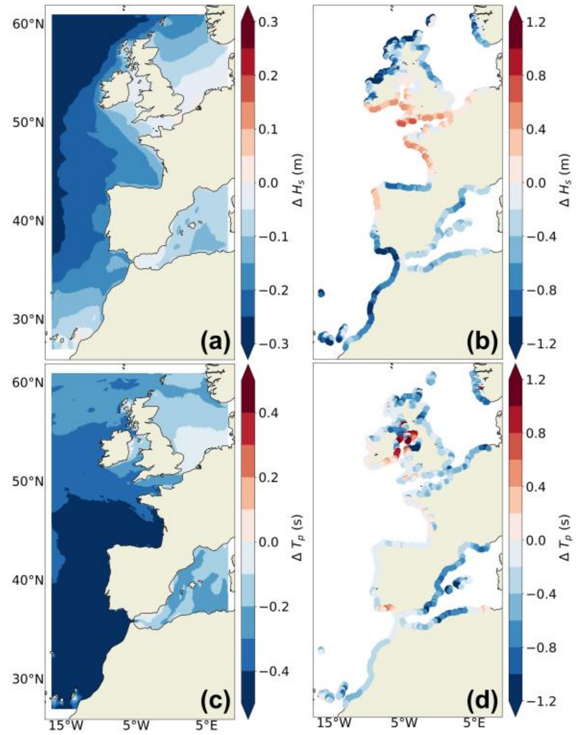

Figure 6: Projected changes in mean (first column) and coastal extreme 1-in-100-year (second column) wave conditions for the 2081-2100 period (relative to 1986-2005) under the ~~SSP1-2.6 (first column) and~~ SSP5-8.5 ~~(second column) scenarios~~climate scenario for (a,b) the significant wave height (Δ~~Hs,~~H_s, in m~~),~~) and (c,d~~),~~) the peak period (Δ~~Tp,~~T_P, in s~~)~~ ~~and (e,f) scaling for wave setup (Δ$\sqrt{H_s L_p}$, in m~~).

Projected changes in ~~the~~mean and extreme significant wave height~~,~~ and peak period ~~and wave setup scaling~~ are illustrated in Figure ~~7~~6 for the end of the century under ~~two climate change scenarios. Projected changes under~~ the SSP5-8.5 climate change scenario. Projected changes are globally consistent with other studies (Lobeto et al., 2021; Melet et al., 2020a; Morim et al., 2019; Aarnes et al., 2017; Casas-Prat et al., 2018) with a large decrease in ~~the~~mean significant wave height~~,~~ and peak period ~~and thus in the wave setup scaling~~ in the Atlantic Ocean and Mediterranean Sea (Fig. ~~7b,d,e). For the SSP5-8.5 scenario, in the south of the domain, projected~~6). Projected changes in the mean peak period can reach ~~-0.5 s which represents~~ a decrease of ~~6 %~~ -0.5 s or -6 % in the southern domain in comparison to the historical period (Fig. 6c)~~.of Figure 4e,~~ For the mean significant wave height, projected changes are largest in the north-western domain and can reach -30 cm or -10 ~~%.~~% (Fig. 6a). Changes in ~~the~~ wave height and peak period result from changes in the wave spectrum composed by different wave regimes (e.g. swells and wind-waves). The large decrease in ~~the~~ significant wave height ~~under the SSP5-8.5 scenario (Fig. 7b)~~ is due to a general decline in ~~the~~ wind speed forcing from ~~CNRM-CM6~~ the global climate model forcing (Tab. 1 ~~HR~~) over the domain and in the North Atlantic Ocean, inducing changes in both wind-waves and swells in the domain (not shown). The decrease in ~~the~~ wind speed under the SSP5-8.5 scenario is consistent with other CMIP6 models projections (Carvalho et al., 2021). ~~In terms of wave setup scaling, projected changes can reach a decrease of 2 m or 6 % under SSP5-8.5 scenario along the north Iberian coasts (Fig. 7f). In terms of sea level equivalent, using parameterization (1) with a beach slope of 4 % and 7 % (Sect. 2.3), the decrease in the wave setup in the deep ocean can reach between -2.8 cm and -4.9 cm. These changes are thus rather small (but not negligible) compared to the projected sea level rise of about +80 cm over the northeastern Atlantic domain (Chaigneau et al., 2022) but are of opposite sign. These changes in wave setup are mainly related to moderate changes in the peak period which is squared in formulation (1): 63 % of the wave setup changes are due to those in peak period and 37 % are due to changes in significant wave height. Except in the North Sea, the spatial patterns of the wave projected changes under the SSP1-2.6 scenario (Fig. 7a,c,e) are broadly the same as under the SSP5-8.5 scenario, but with an overall smaller magnitude.~~

~~**Extreme projections: 99th percentile**~~

Mis en forme : Police :10 pt, Couleur de police : Automatique

Mis en forme : Police :10 pt, Couleur de police : Automatique (×9)

Mis en forme : Couleur de police : Automatique (×33)

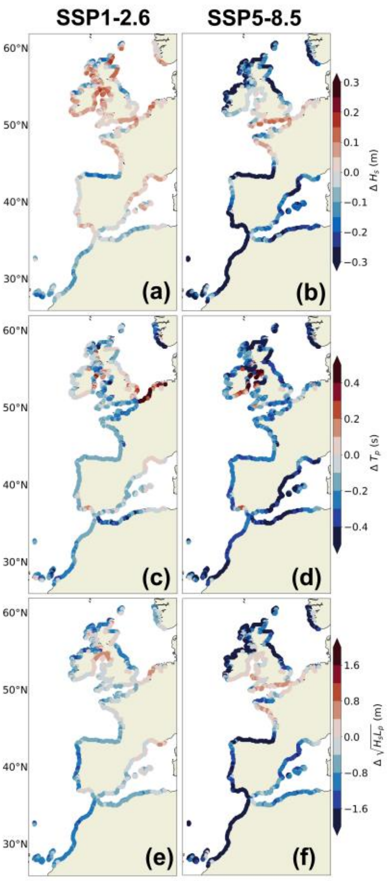

Figure 8: Projected changes in **incoming extreme (99th percentile) waves conditions for** the **2081-2100 period (relative to 1986-2005) under the SSP1-2.6 (first column) and SSP5-8.5 (second column) scenarios in IBI-CCS-WAV for (a,b) significant wave height (ΔHs, in m), (c,d) peak period (ΔTp, in s) and (e,f) scaling for wave setup (Δ$\sqrt{H_s L_p}$, in m).**

Projected changes in the 99th percentile of significant wave height, peak period and wave setup scalingextremes are illustrated in Figure 8 for the end of the century under two climate change scenarios. Changes in the 99th percentile of peak period are moderate as it generally represents a decrease of less than 2.5 % for the SSP5-8.5 scenario (Fig. 8c,d). For the significant wave height, projected changes in the 99th percentile under SSP5-8.5 scenario are large with a decrease of more than 30 cm or 12 % in the southern part of the domain. For both scenarios, projected changes in the 99th percentile of significant wave height are quitespatially substantially different from those in the mean state, as reported in Morim et al., 2018. This is associated with different changes in the extreme wind speed forcing compared to those in the mean state (not shown). For example, for the SSP5-8.5 scenario, thea large decrease in the extreme wind speed (Fig. 3bA2b) and thus in the significant wave height of more than 1 m or 12 % is located in the North Atlantic south of 45 °N and north of 55 °N (Fig. 7b6b). This is consistent with other studies (Aarnes al., 2017; Meucci et al., 2021) in which the largest decrease in the 99th percentile of extreme significant wave height is also found in the southern domain (Fig. 8b).. In the English Channel, Celtic Sea and French Atlantic coasts, the model even exhibits an increase in the extreme significant wave height that has not been reported in other studies for both scenarios (Fig. 8a,b).. This increase is however consistent with projected changes in extreme wind speed shown in Fig. 3bFigure A2b for the English Channel. In the Mediterranean Sea, the SSP5-8.5 and SSP1-2.6 scenarios exhibit significant wave height projected changes of a different sign (Fig. 8a,b) associated with different projected changes in for the forcing global climate model. Projected changes in the extreme winds (not shown). Over the whole domain, as projected changes in extreme peak periods are small, projected changes in extreme wave setup scaling are mostly governed by those in extreme significant wave height (Fig. 8e,f) in contrast to the projected changes in mean state of Figure 7. For instance, along the north Iberian coasts, projected changes in wave setup scaling show a decrease of 2 m or 4 %, with 70 % of the changes due to those in significant wave height and 30 % due to changes in peak period. In terms of sea level equivalent, the decrease in extreme wave setup can

Mis en forme : Police :10 pt, Non Gras, Couleur de police : Automatique

Mis en forme : Police :10 pt, Non Gras, Couleur de police : Automatique

Mis en forme : Couleur de police : Automatique

Mis en forme : Couleur de police : Automatique

Mis en forme : Couleur de police : Automatique

Mis en forme : Couleur de police : Automatique

Mis en forme : Couleur de police : Automatique

Mis en forme : Couleur de police : Automatique

Mis en forme : Couleur de police : Automatique

Mis en forme : Couleur de police : Automatique

Mis en forme : Couleur de police : Automatique

Mis en forme : Couleur de police : Automatique

Mis en forme : Couleur de police : Automatique

Mis en forme : Couleur de police : Automatique

Mis en forme : Couleur de police : Automatique

Mis en forme : Couleur de police : Automatique

reach between -2.8 cm and -4.9 cm using (1), as for the mean state of Figure 7. peak period are moderate as they generally represent a decrease of less than 2.5 % (Fig. 6d).

Mis en forme : Couleur de police : Automatique

3.2.2 Projected changes in wave roses

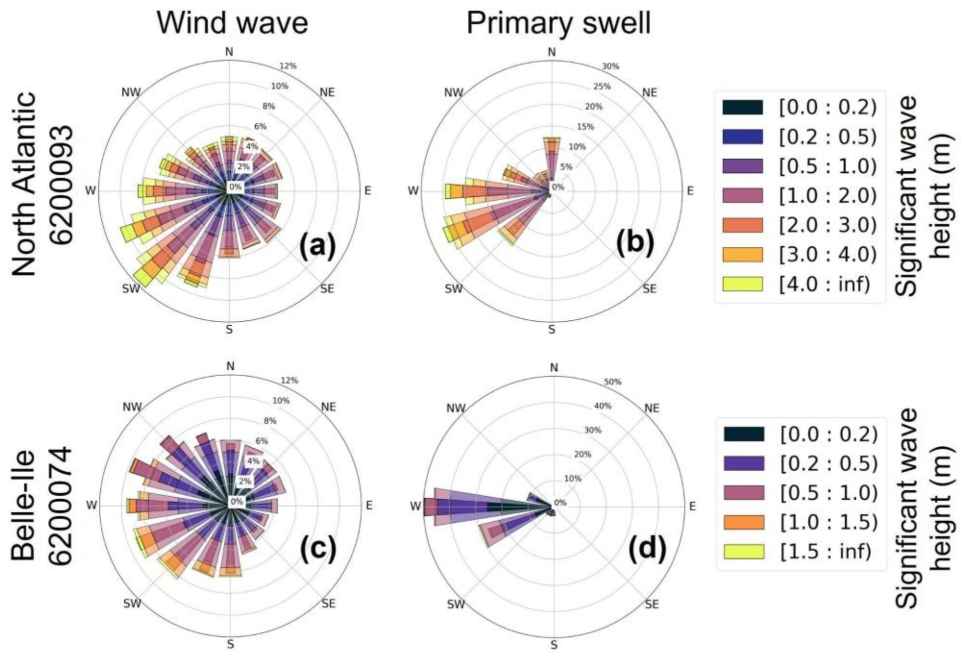

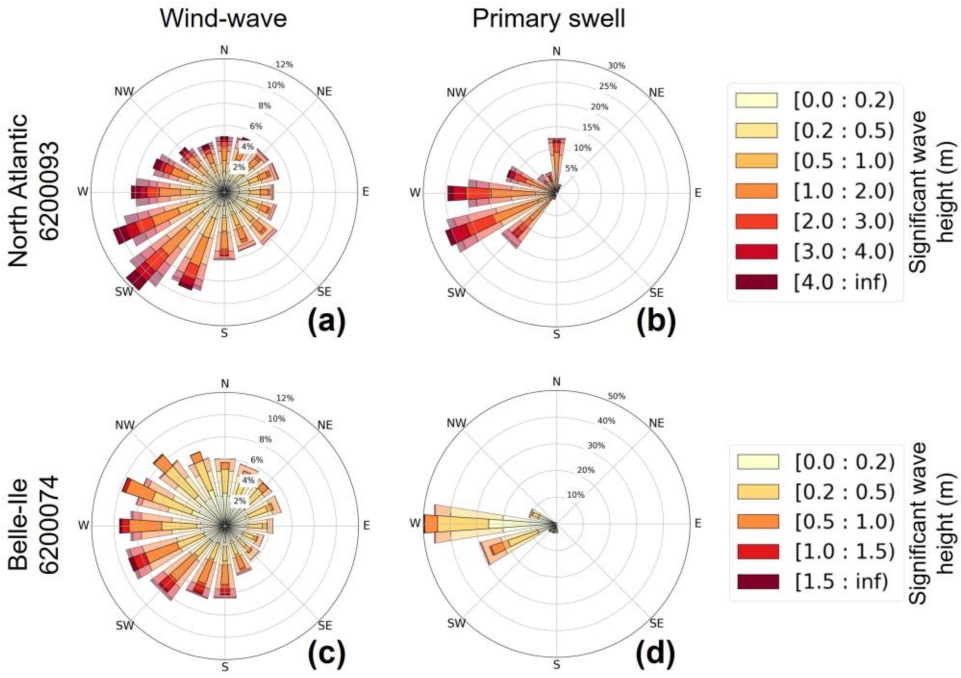

Figure 97: Projected changes (SSP5-8.5 scenario) in directional distribution of significant wave height for the 2081-2100 period (narrow angle bins, dark colors) relative to 1986-2005 (wide angle bins, pale colors) in IBI-CCS-WAV at

Mis en forme : Police :10 pt, Couleur de police : Automatique

Mis en forme : Police :10 pt, Couleur de police : Automatique

star locations of Fig. ~~2a~~1a: North Atlantic buoy 6200093 (first row~~),~~) and Belle-Ile buoy 6200074 (second row). The significant wave height and mean wave direction have been classified according to their origin: wind~~-~~wave (a,c) and primary swell (b,d). Colors indicate wave height distribution in each direction bin.

Projected changes in ~~the~~ directional wave height distributions are ~~shown~~presented on wave roses at the two locations validated in ~~Figure 6.~~Sect. 3.1 (Fig. 7). The wave roses ~~have been~~are decomposed into ~~the~~ wind~~-~~wave and primary swell contributions. The ~~significant wave height~~ roses due to the primary swell contribution (Fig. ~~9b~~7b,d) are very close to ~~the significant wave height roses~~those of ~~Fig. 6~~Figure 5, showing that ~~most waves are due to~~ the primary swell ~~at this location.~~is the main contributor to significant wave height in the Atlantic Ocean. At ~~Belle-Ile buoy 6200074~~the end of the century, the wave rose at the Belle-Ile buoy exhibits a ~~change~~clockwise shift of 20 ° in the main direction of the wind-wave ~~under the SSP5-8.5 scenario (Fig. 9c). Over the historical period, the main direction is~~ , changing from a west-southwest ~~whereas it would be shifted clockwise~~ to a west-northwest direction (~~20 °) at the end of the century under the SSP5-8.5 scenario (Fig. 9c~~Fig. 7c). In this zone, a clockwise shift in the wave direction has already been documented in Morim et al., 2019. This shift seems to come mainly from small waves with significant wave height less than 50 cm. For the primary swell at Belle-Ile, we observe a slight strengthening of the swell from the west direction~~, and thus~~ associated with a reduction of the wave components coming from the southwest (Fig. ~~9d). The results~~ 7d). Projected changes are ~~quite~~ different for North Atlantic buoy ~~6200093. Projected changes exhibit~~showing a slight strengthening of the wind-wave heights in the southwest, west-southwest direction bins ~~with an~~ (Fig. 7a) and a larger strengthening (occurrence increased by ~~a few percent (Fig. 9a). Also, for North Atlantic buoy 6200093, the projected changes in the~~ 5%) of the primary swell ~~are larger than at Belle-Ile buoy 6200074. The occurrence of the~~ heights in the west direction ~~has increased by 5 %~~ (Fig. ~~9b). Finally, a slight decrease in swells with significant wave heights of more than 4m is found under the SSP5-8.5 scenario for the west and west-northwest directions (Fig. 9b).~~ 7b).

In ~~Sect. 3.2, as reported in other studies~~summary, we ~~observed~~observe a general decrease in mean and extreme significant wave height and peak period over the domain ~~and~~as well as a clockwise mean wave direction change along the French Atlantic coasts. ~~As IBI-CCS-WAV seems to be representative of other studies, we can used it to~~These projected changes are coherent with previous studies.

4 Results: Impact of the non-linear interaction of sea level on waves considered in the regional wave model

We now assess the methodological ~~modelling questions such as~~ question of the impact on wave characteristics of considering ~~the~~ hourly ~~waters~~sea level variations ~~on the wave model~~in the regional wave model. For that purpose, the two simulations that do and do not account for the non-linear interaction of sea level on waves (IBI-CCS-WAV and IBI-CCS-WAV_ssh respectively) are compared in terms of significant wave height and peak period for both the mean state and extreme events.

Mis en forme : Police :10 pt, Couleur de police : Automatique
Mis en forme : Police :10 pt, Couleur de police : Automatique
Mis en forme : Police :10 pt, Couleur de police : Automatique
Mis en forme : Couleur de police : Automatique, Anglais (États-Unis)
Mis en forme : Couleur de police : Automatique
Mis en forme : Couleur de police : Automatique
Mis en forme : Couleur de police : Automatique
Mis en forme : Couleur de police : Automatique
Mis en forme : Couleur de police : Automatique
Mis en forme : Couleur de police : Automatique
Mis en forme : Couleur de police : Automatique
Mis en forme : Couleur de police : Automatique
Mis en forme : Couleur de police : Automatique
Mis en forme : Couleur de police : Automatique
Mis en forme : Couleur de police : Automatique
Mis en forme : Couleur de police : Automatique
Mis en forme : Couleur de police : Automatique
Mis en forme : Couleur de police : Automatique
Mis en forme : Couleur de police : Automatique
Mis en forme : Couleur de police : Automatique
Mis en forme : Couleur de police : Automatique
Mis en forme : Couleur de police : Automatique
Mis en forme : Couleur de police : Automatique
Mis en forme : Couleur de police : Automatique
Mis en forme : Couleur de police : Automatique
Mis en forme : Couleur de police : Automatique
Mis en forme : Couleur de police : Automatique
Mis en forme : Couleur de police : Automatique
Mis en forme : Couleur de police : Automatique
Mis en forme : Couleur de police : Automatique
Mis en forme : Couleur de police : Automatique
Mis en forme : Couleur de police : Automatique
Mis en forme : Couleur de police : Automatique
Mis en forme : Couleur de police : Automatique
Mis en forme : Couleur de police : Automatique
Mis en forme : Couleur de police : Automatique
Mis en forme : Couleur de police : Automatique
Mis en forme : Couleur de police : Automatique
Mis en forme : Couleur de police : Automatique
Mis en forme : Couleur de police : Automatique
Mis en forme : Couleur de police : Automatique
Mis en forme : Couleur de police : Automatique
Mis en forme : Couleur de police : Automatique
Mis en forme : Couleur de police : Automatique

~~4 Impact of non-linear wave-water level interactions accounted for in the regional wave model~~

4.1 Impact for the entire coastal domain

Mis en forme : Couleur de police : Automatique

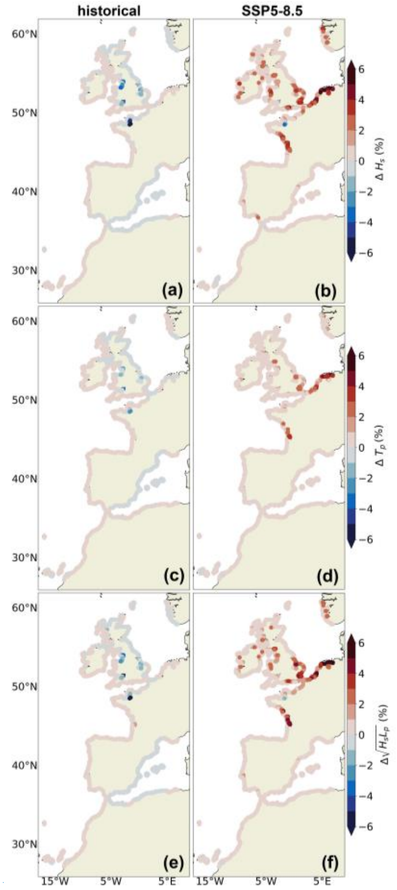

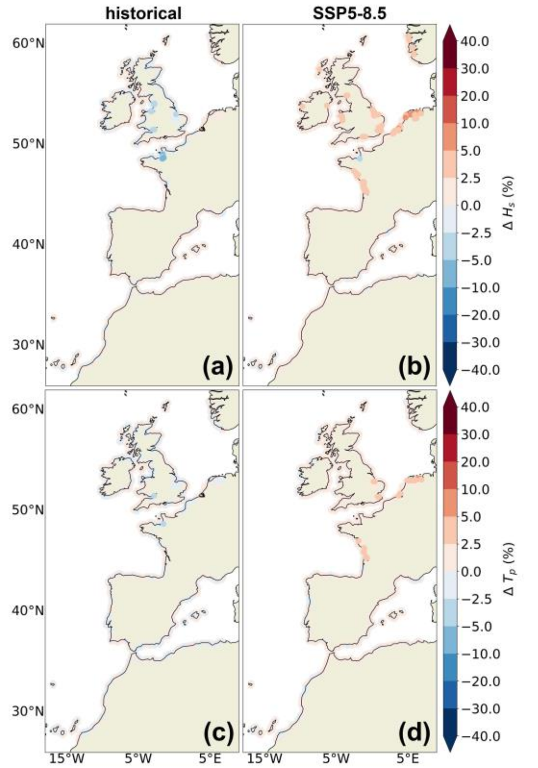

Figure ~~10~~8: Impact of the inclusion of ~~the~~ hourly ~~water~~sea level variations in the wave model on the mean state of (a,b) significant wave height (first row, Δ~~Hs,~~H_s, in ~~%),~~%) and (c,d) peak period (second row, Δ~~Tp, in %) and (e,f) wave setup scaling (third row, Δ$\sqrt{H_s L_p}$~~ T_P, in %). The first column shows the relative differences of mean state between IBI-CCS-WAV_ssh and IBI-CCS-WAV for the 1986-2005 period. The second column shows the relative differences of mean state between IBI-CCS-WAV_ssh and IBI-CCS-WAV for the 2081-2100 period under the SSP5-8.5 scenario. Note that the color bars of Figure 8 and 9 are not linear and are identical to facilitate the comparisons between the two figures.

~~The impact of accounting for hourly water level variations in the wave model on the mean state of wave conditions is shown in Figure 10 by comparing IBI-CCS-WAV_ssh to IBI-CCS-WAV. Except for a few places, like in~~Except for a few locations, such as the Bay of Mont-Saint-Michel or the mouth of some rivers in the United Kingdom, the impact of including ~~the water~~sea level variations ~~on~~in the wave model has almost no impact on ~~average as shown in~~ the ~~first column~~mean state of waves conditions for the historical period (Fig. ~~10.~~8a,c). This suggests that there ~~are~~is no strong non-linear ~~effects between waves and water~~effect of sea level on waves that would make ~~an impact~~a difference on the 20-year mean state ~~on average~~ for the majority of the coastal domain with our model settings.

~~Differences in the wave projections due to the inclusion of hourly water level changes are illustrated in the second column of Fig. 10 at~~ At the end of the century ~~(2081-2100) under the SSP5-8.5 scenario. Sea level~~, projected sea level changes in the ~~IBI-CCS~~regional ocean ~~model during the 21st century~~simulations used as forcing (Tab. 1, Sect. 2.3) are mainly dominated by the mean sea level rise~~,~~ (sterodynamic and barystatic sea level rise), with rather small changes in tides and storm surges (Chaigneau et al., 2022). ~~Therefore, as IBI-CCS-WAV and IBI-CCS-WAV_ssh are forced by the same winds, Figure 10 mostly shows the impact of mean sea level rise on waves, even if not completely linear. In IBI-CCS, the mean sea level rise averaged over the IBI domain reaches~~ This increase reaches approximately +80 cm in our region in 2100 compared to the 1986-2005 period under the SSP5-8.5 scenario ~~considering changes in tides and storm surges too (Chaigneau et al., 2022). Until the end of the paper, the mean sea level rise term will also consider projected changes in the mean state of tides~~. Therefore, since IBI-CCS-WAV and IBI-CCS-WAV_ssh are forced by the same winds and ~~storm surges.~~thus the same storms, Figure 8 mainly shows the impact of mean sea level rise on the mean wave conditions. This long-term mean sea level rise has an overall small effect on the ~~coastal points of the~~ large continental shelf where shallow and intermediate water dynamics ~~prevail~~predominate (Fig. ~~2a). The~~1a). Future mean significant wave ~~height projections~~heights are up to +38 % (+4 cm ~~larger (e.g. +6 % larger~~) higher in IBI-CCS-WAV_ssh than in IBI-CCS-WAV~~)~~ along the French Atlantic coasts and in the southern North Sea (Fig. ~~10b~~8b).

Mis en forme : Police :10 pt, Couleur de police : Automatique
Mis en forme : Police :10 pt, Couleur de police : Automatique
Mis en forme : Police :10 pt, Couleur de police : Automatique
Mis en forme : Police :10 pt, Couleur de police : Automatique
Mis en forme : Police :10 pt, Couleur de police : Automatique
Mis en forme : Police :10 pt, Couleur de police : Automatique
Mis en forme : Police :10 pt, Couleur de police : Automatique
Mis en forme : Police :10 pt, Couleur de police : Automatique
Mis en forme : Couleur de police : Automatique
Mis en forme : Couleur de police : Automatique
Mis en forme : Couleur de police : Automatique
Mis en forme : Couleur de police : Automatique
Mis en forme : Couleur de police : Automatique
Mis en forme : Couleur de police : Automatique
Mis en forme : Couleur de police : Automatique
Mis en forme : Couleur de police : Automatique
Mis en forme : Couleur de police : Automatique
Mis en forme : Couleur de police : Automatique
Mis en forme : Couleur de police : Automatique
Mis en forme : Couleur de police : Automatique
Mis en forme : Couleur de police : Automatique
Mis en forme : Couleur de police : Automatique
Mis en forme : Couleur de police : Automatique
Mis en forme : Couleur de police : Automatique
Mis en forme : Couleur de police : Automatique
Mis en forme : Couleur de police : Automatique
Mis en forme : Couleur de police : Automatique
Mis en forme : Couleur de police : Automatique
Mis en forme : Couleur de police : Automatique
Mis en forme : Couleur de police : Automatique, Anglais (Royaume-Uni)
Mis en forme : Couleur de police : Automatique
Mis en forme : Couleur de police : Automatique

This result ~~agrees~~is consistent with Arns et al., 2017 who showed that changes in water depth ~~changes~~ induced by sea level rise ~~were leading to waves of~~ resulted in greater ~~amplitude and period, breaking closer to the shore.~~wave amplitudes near the coast. The impact of ~~the~~ sea level ~~rise~~ on ~~the mean state of significant wave height leads to an impact of the same order of magnitude (up to +6 %) on the wave setup scaling mean state (Fig. 10f). For the peak period, the impact is moderate (Fig. 10d).~~future mean peak periods is even smaller, with differences up to + 4% (or 0.05 s) (Fig. 8d). In the southern North Sea, projected changes in both significant wave height and peak period are small (~~Fig 7b) and therefore an added impact of +3 cm due to the sea level rise corresponds to more than 70 % of the projected total changes under SSP5-8.5 scenario.~~

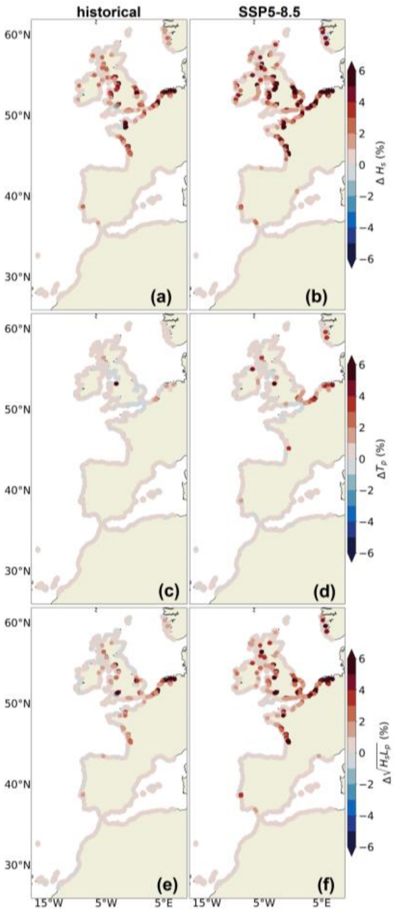

Figure ~~11~~6a). The small impact of the non-linear interaction of sea level on waves (+3 cm, + 0.05 s) therefore represents more than 70% of the future change.

Mis en forme : Couleur de police : Automatique

Mis en forme : Couleur de police : Automatique

Mis en forme : Couleur de police : Automatique

Mis en forme : Couleur de police : Automatique

Mis en forme : Couleur de police : Automatique

Mis en forme : Couleur de police : Automatique

Mis en forme : Couleur de police : Automatique

Mis en forme : Couleur de police : Automatique

Mis en forme : Couleur de police : Automatique

Mis en forme : Couleur de police : Automatique

Mis en forme : Couleur de police : Automatique

Mis en forme : Police :10 pt, Non Gras, Couleur de police : Automatique

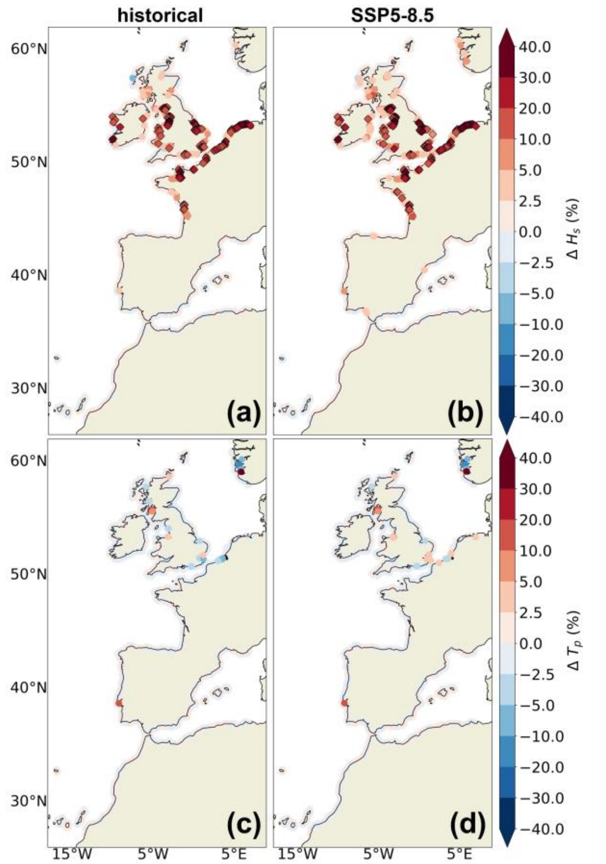

Figure 9: Impact of the inclusion of ~~the~~ hourly ~~water~~sea level variations in the wave model on the ~~99th percentile~~ 1-in-100-year return level of (a,b) significant wave height (first row, Δ~~Hs,~~H_S, in ~~%),~~%) and (c,d) peak period (second row, Δ~~Tp, in %) and (e,f) wave setup scaling (third row, Δ$\sqrt{H_s L_p}$~~ T_P, in %). The first column shows the relative differences of the ~~99th percentile~~ 1-in-100-year return level between IBI-CCS-WAV_ssh and IBI-CCS-WAV for the 1986-2005 period. The second column shows the relative differences of the ~~99th percentile~~1-in-100-year return level between IBI-CCS-WAV_ssh and IBI-CCS-WAV for the 2081-2100 period under the SSP5-8.5 scenario. The large diamonds represent the locations where the differences between both simulations are significant (i.e. where the confidence intervals associated with the 100-year return level calculation are disjoint). Note that the color bars ~~are saturated in red for some points for (a), (b)~~ of Figure 8 and 9 are not linear and ~~(f).~~are identical to facilitate the comparisons between the two figures.

~~The impact of accounting for the hourly water level variations in the wave model on the 99th percentile is shown in Figure 11 by comparing IBI-CCS-WAV_ssh to IBI-CCS-WAV. The impact~~Considering extreme events, the impact of sea level on significant wave heights over the historical period is substantially more important ~~when considering the 99th percentile instead of the mean state~~ (Fig. ~~11, first column~~9a). The coastal points of the ~~large~~wide continental shelf are ~~quite~~significantly impacted (southern North Sea, English Channel, seas around the United Kingdom, French Atlantic coasts~~) and~~). This is particularly the case for macro-tidal locations (Fig. ~~2b~~1b) such as the Bay of Mont-Saint-Michel, the Bristol Channel and the eastern Irish Sea. In these areas, the historical ~~99th percentile~~1-in-100-year event of significant wave height ~~and wave setup scaling~~ is up to +~~8% and +6 %~~ 30 % (+40 cm) higher ~~respectively~~ when considering ~~water~~sea level variations, mostly dominated by tidal variations~~.~~

~~The~~, as discussed in Sect. 4.2. At the end of the century, the impact of including ~~the~~ hourly ~~water~~sea level variations on the ~~projections of the 99th percentile is larger due to the combination of the impact of tidal range and mean sea level rise. For the significant wave height, the projected 99th percentile is increased by up to +6 cm or +10 % and for the wave setup scaling it represents an increase of up to +8 % (Fig. 11 second column). As projected changes in the~~future 1-in-100-year level wave events is even larger mostly due to the combined effect of the tides and mean sea level rise. Future extreme significant wave

Mis en forme : Police :10 pt, Couleur de police : Automatique
Mis en forme : Police :10 pt, Couleur de police : Automatique
Mis en forme : Police :10 pt, Couleur de police : Automatique
Mis en forme : Police :10 pt, Couleur de police : Automatique
Mis en forme : Police :10 pt, Couleur de police : Automatique
Mis en forme : Police :10 pt, Couleur de police : Automatique
Mis en forme : Police :10 pt, Couleur de police : Automatique
Mis en forme : Police :10 pt, Couleur de police : Automatique
Mis en forme : Police :10 pt, Couleur de police : Automatique
Mis en forme : Police :10 pt, Couleur de police : Automatique
Mis en forme : Police :10 pt, Couleur de police : Automatique
Mis en forme : Couleur de police : Automatique
Mis en forme : Couleur de police : Automatique
Mis en forme : Couleur de police : Automatique
Mis en forme : Couleur de police : Automatique
Mis en forme : Couleur de police : Automatique
Mis en forme : Couleur de police : Automatique
Mis en forme : Couleur de police : Automatique
Mis en forme : Couleur de police : Automatique
Mis en forme : Couleur de police : Automatique
Mis en forme : Couleur de police : Automatique
Mis en forme : Couleur de police : Automatique
Mis en forme : Couleur de police : Automatique
Mis en forme : Couleur de police : Automatique
Mis en forme : Espace Avant : 12 pt, Après : 12 pt
Mis en forme : Couleur de police : Automatique
Mis en forme : Couleur de police : Automatique
Mis en forme : Couleur de police : Automatique
Mis en forme : Couleur de police : Automatique

heights ~~and peak periods in IBI-CCS-WAV are quite small at the coast (Fig. 8b,c), especially on the French Atlantic coasts and on the North Sea coasts (<10 cm, <0.3 s), an impact of the hourly water level variations of +6 cm~~are increased by up to +40 % or +~~0.1 s represents more than 80 % of the projected changes in IBI-CCS-WAV_ssh. These results highlight that wave-water level non-linear interactions should be considered for applications on wave extreme events in particular in coastal zones subject to large water level variations or on large continental shelves, with implications for estimates of both past and future sea level changes.~~ 60 cm (Fig. 9b). On the contrary, extreme peak periods are negligibly impacted by the non-linear interaction of sea level on waves (Fig. 9c,d).

4.2 ~~Impact~~Example of the impact on extreme events at two specific locations~~: Bay of Mont-Saint-Michel and French Atlantic coast~~

The largest impact of including ~~water~~sea level variations ~~for~~in the wave ~~modeling~~model is found during extreme events, as shown in Figure ~~11. In Sect. 4.2, the~~9. We now focus ~~is~~ on two specific French regions where an impact ~~of non-linear wave-water level interactions on the wave extremes~~ has been identified in ~~Figures 11~~Figure 9. In the Bay of Mont-Saint-Michel, strong hourly ~~water~~sea level variations occur due to the large tidal range in the region (~~about~~ 10 ~~meters~~m, Fig. ~~2b~~1b). For the French Atlantic coast, the tidal range is large (4 ~~meters~~m, Fig. ~~2b~~1b) but smaller than in the Bay of Mont-Saint-Michel.

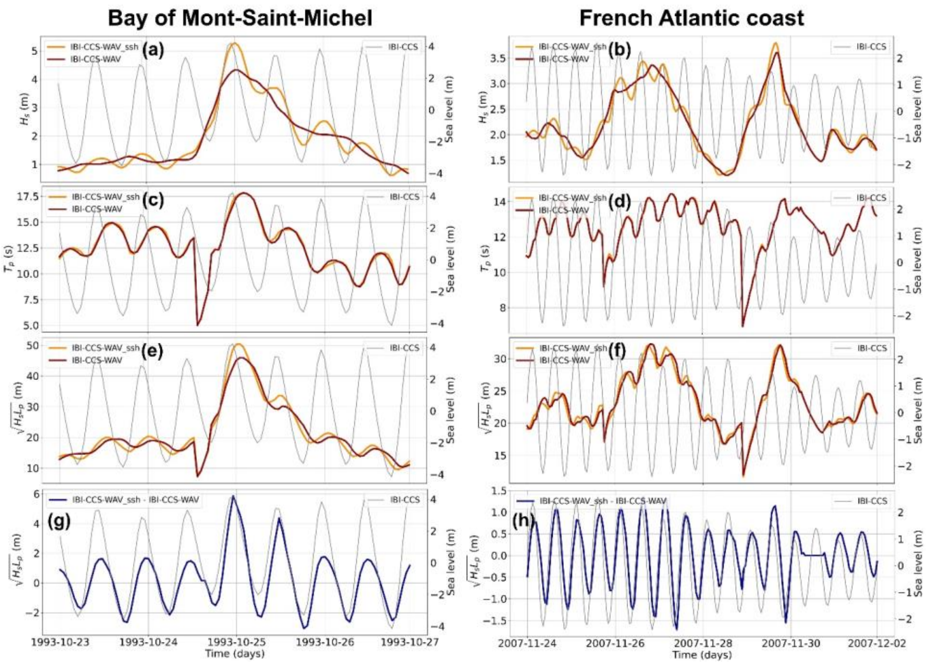

Mis en forme : Couleur de police : Automatique

Mis en forme : Couleur de police : Automatique, Anglais (États-Unis)

Mis en forme : Couleur de police : Automatique

Mis en forme : Couleur de police : Automatique

Mis en forme : Couleur de police : Automatique

Mis en forme : Couleur de police : Automatique

Mis en forme : Couleur de police : Couleur personnalisée(RVB(28;29;30))

Mis en forme : Couleur de police : Automatique

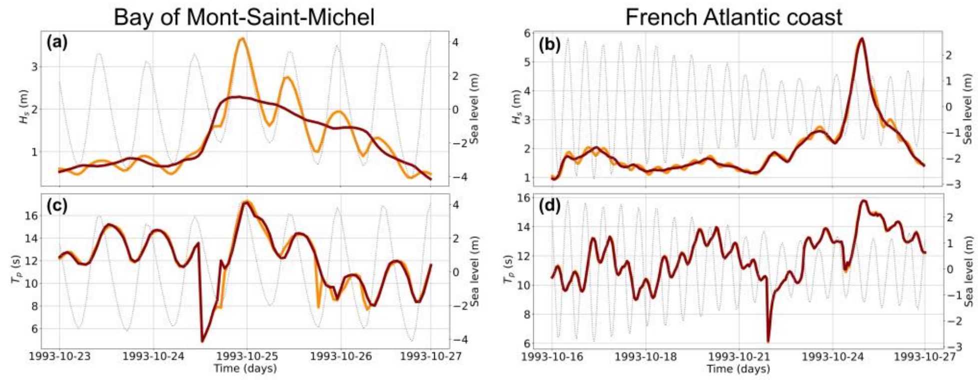

Figure ~~12~~10: Time series of incoming wave conditions for the Bay of Mont-Saint-Michel (first column) and for the French Atlantic coast (second column) during an extreme significant wave height event~~.~~ of October 1993. The two locations are marked on Fig. ~~2b~~1b. The curves represent IBI-CCS-WAV (dark red curve) and IBI-CCS-WAV_ssh (dark yellow curve) ~~and 3 variables are displayed:~~for (a,b) the significant wave height (~~Hs,~~H_S, in m), and (c,d) the peak period (~~Tp,~~T_P, in s~~), (e,f) scaling for wave setup ($\sqrt{H_s L_p}$, in m) and (g,h) differences in the wave setup scaling between the two simulations. Water~~). Sea level variations are shown in thin ~~gray~~grey dotted lines, with the right y-axis on each panel.

Time-series of significant wave height~~,~~, and peak period~~, wave setup scaling and differences in the wave setup scaling for two~~ during an extreme significant wave height ~~events~~event are ~~illustrated~~shown in Figure ~~12. The events selected in the model did not actually occur since~~10. Note that as the global climate model forcing is not in phase with ~~the observed forcing.~~observation in terms of internal climate variability, the event selected cannot be compared directly to observations. Nevertheless, we have validated in section 3.1 that the amplitude of simulated extreme events was realistic. The significant wave height ~~and wave setup scaling~~ time~~-~~ series from IBI-CCS-WAV_ssh oscillate hourly, in phase with the tide~~ in IBI-CCS-WAV_ssh~~, illustrating the consideration of hourly ~~water~~sea levels in the regional wave model (Fig. ~~12a~~10a,b~~,e,f~~). In the case of the Bay of Mont-Saint-Michel, ~~due to~~ the ~~large tidal range, the highest~~largest significant wave height~~,~~ reached on day 25/10/1993 ~~during~~at high tide~~,~~ is 1 m ~~larger (+25~~higher (+30 %) in IBI-CCS-WAV_ssh than in IBI-CCS-WAV~~. The impact of the water level variations on the peak period is however almost zero~~ due to the large tidal range (Fig. ~~12c). In both IBI-CCS-WAV and IBI-CCS-WAV_ssh, diurnal variations of the peak period appear due to tidal current that shortens or lengthens the dominant wave period (Ardhuin et al., 2012). The impact of the inclusion on the wave model of the hourly water level variations on the wave setup scaling (Fig. 12e) is balanced by the effects on the significant wave height and peak period of the water level variations. For the peak of day 25/10/1993, the differences of the wave setup scaling between IBI-CCS-WAV and IBI-CCS-WAV_ssh can reach 6 meters (Fig. 12g). Differences in the wave setup can reach +8.4 cm to +14.7 cm for the peak event using parameterization (1) with beach slopes of 4 % and 7 %.~~10a). As the Bay of Mont Saint-Michel has one of the highest tidal ranges in the IBI domain, the ~~impacts found correspond~~observed impact of sea level variations on waves corresponds to the upper ~~bound~~limit with the ~~settings~~parameters of our model.

For the French Atlantic coast, ~~due to a lower tidal range of 4 meters, the impact of including the~~in this specific case, the extreme event of significant wave height occurs at low tide during a medium neap tide so the impact of hourly ~~water~~sea level variations on the extreme ~~wave conditions is less important (Fig. 12, second column). For the event of 29/11/2007, differences between IBI-CCS-WAV_ssh and IBI-CCS-WAV are of +25 cm (+6%) for the~~ significant wave height ~~and of +1 m (+3 %) for the wave setup scaling (Fig. 12b,f). In terms of wave setup, this would result in differences between +1.4 cm and +2.45 cm with parameterization (1) which is substantially lower than in the Bay of Mont-Saint-Michel.~~

~~However~~is null. In both cases, it can be pointed out that the ~~most significant~~ increase in wave height occurs ~~in both cases~~ at high tide. These results are in agreement with Lewis et al., 2019 and Calvino et al., 2022 who both showed a significant increase in wave height at high tide at a finer scale. In Calvino et al., 2022, this impact seems to be explained mainly by the effect of bottom friction, which is less important at high tide as ~~there is more water. In our case, additional analyses would be needed to understand which is the primary process included in the model (Sect. 2.1) responsible for the non-linear interactions.~~the water column is higher. In the case of Arns et al. 2017, waves are higher when sea level increases (e.g. at high tide) because they break closer to the shore. In our case, additional analyses would be needed to understand which process included in the model (Sect. 2.1) is the most responsible for the non-linear interaction of sea level on significant wave height. In both IBI-CCS-WAV and IBI-CCS-WAV_ssh, diurnal variations of the peak period appear due to tidal current that shortens or lengthens the dominant wave period (Ardhuin et al., 2012) but the impact of sea level variations is almost null (Fig. 10c,d).

Mis en forme : Police :10 pt, Couleur de police : Automatique
Mis en forme : Police :10 pt, Couleur de police : Automatique
Mis en forme : Police :10 pt, Couleur de police : Automatique
Mis en forme : Police :10 pt, Couleur de police : Automatique
Mis en forme : Police :10 pt, Couleur de police : Automatique
Mis en forme : Police :10 pt, Couleur de police : Automatique
Mis en forme : Police :10 pt, Couleur de police : Automatique
Mis en forme : Police :10 pt, Couleur de police : Automatique
Mis en forme : Police :10 pt, Couleur de police : Automatique
Mis en forme : Police :10 pt, Couleur de police : Automatique
Mis en forme : Police :10 pt, Couleur de police : Automatique
Mis en forme : Police :10 pt, Couleur de police : Automatique
Mis en forme : Police :10 pt, Gras, Couleur de police : Automatique, Anglais (États-Unis), Surlignage
Mis en forme : Couleur de police : Couleur personnalisée(RVB(28;29;30))
Mis en forme : Couleur de police : Couleur personnalisée(RVB(28;29;30))
Mis en forme : Couleur de police : Couleur personnalisée(RVB(28;29;30))
Mis en forme : Couleur de police : Couleur personnalisée(RVB(28;29;30))
Mis en forme : Couleur de police : Couleur personnalisée(RVB(28;29;30))
Mis en forme : Couleur de police : Automatique
Mis en forme : Couleur de police : Automatique
Mis en forme : Couleur de police : Couleur personnalisée(RVB(28;29;30))
Mis en forme : Couleur de police : Automatique
Mis en forme : Couleur de police : Automatique
Mis en forme : Couleur de police : Automatique
Mis en forme : Couleur de police : Automatique
Mis en forme : Couleur de police : Automatique
Mis en forme : Couleur de police : Automatique
Mis en forme : Couleur de police : Automatique
Mis en forme : Couleur de police : Automatique
Mis en forme : Couleur de police : Automatique
Mis en forme : Couleur de police : Automatique
Mis en forme : Couleur de police : Automatique
Mis en forme : Couleur de police : Automatique
Mis en forme : Couleur de police : Automatique
Mis en forme : Couleur de police : Automatique
Mis en forme : Couleur de police : Automatique
Mis en forme : Couleur de police : Automatique
Mis en forme : Couleur de police : Automatique
Mis en forme : Couleur de police : Automatique
Mis en forme : Couleur de police : Automatique

4.3 Impact on extreme events in terms of return periods

It was shown in Sect. 4.1 that the impact of the inclusion of the hourly water level variations in the wave model had a larger effect on the 99th percentile than on the mean state of wave conditions. To better document the impacts on extreme events, we now focus on high return periods, such as the 100-year return level. In Sect. 4.3, a nonstationary extreme value analysis (EVA) is performed for each location time series by using the approach described by Mentaschi et al., 2016. This method is used to detect long-term trends in the extremes and to filter out the variability on time scales shorter than 30 years. For each location and wave time series, the output of the EVA analysis is a time-varying generalized Pareto distribution (GPD).

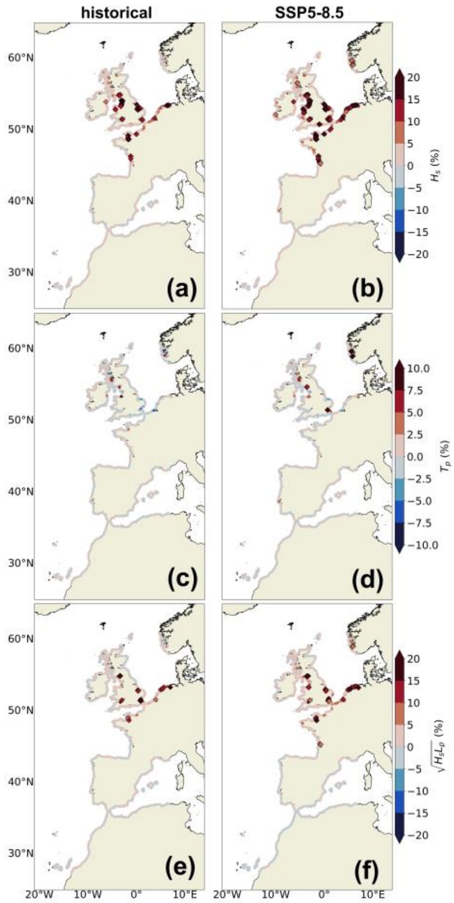

Figure 13: Impact of the inclusion of the hourly water level variations in the wave model on the 100-year return level of (a,b) significant wave height (first row, ΔHs, in %), (c,d) peak period (second row, ΔTp, in %) and (e,f) wave setup scaling (third row, $\Delta\sqrt{H_s L_p}$, in %). The first column shows the relative differences of the 100-year return level between IBI-CCS-WAV_ssh and IBI-CCS-WAV for the year 1985 (representative of the 1970-2000 period). The second column shows the relative differences of the 100-year return level between IBI-CCS-WAV_ssh and IBI-CCS-WAV for the year 2085 (representative of the 2070-2100 period) under the SSP5-8.5 scenario.

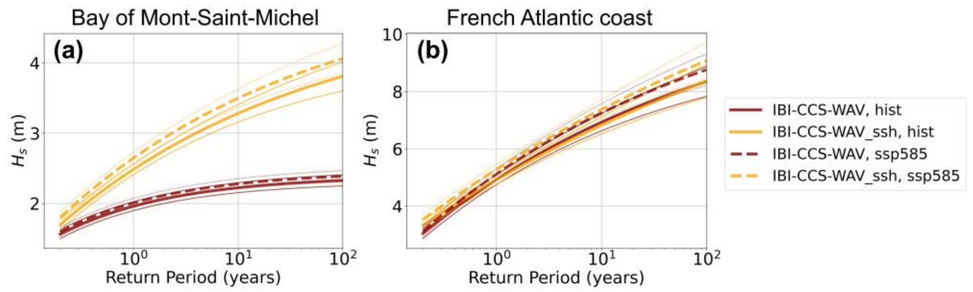

The large diamonds represent the locations where the differences between both simulations are significant (i.e. where the confidence intervals associated with the 100-year return level calculation are disjoint). Note that the colorbars are saturated in red for some points for (b).

Projected changes in the 100-year return level under SSP5-8.5 scenario (not shown) are globally consistent with projected changes in the 99th percentile of significant wave height, peak period and wave setup scaling of Figure 8. Therefore, we use the IBI-CCS-WAV and IBI-CCS-WAV_ssh simulations to assess the influence of the inclusion of hourly water level variations in the wave model during high return period events. As for the 99th percentile, the coastal points of the large continental shelf of Figure 13 are highly impacted and particularly macro-tidal locations (Fig. 2b). However, the differences between IBI-CCS-WAV and IBI-CCS-WAV_ssh for the 100-year return level are of a larger amplitude than the differences for the 99th percentile of **Figure 11** for the whole domain. At the end of the century, the consideration in the wave model of the combination of the tidal range, storm surges and mean sea level rise lead to greater values in extreme significant wave height and wave setup scaling by up to +20 % and +10 % respectively. However, these large impacts are found in locations where the projected changes for the 21st century are generally small since the largest projected changes are located in the southern domain. In spite of this, the effect of sea level on waves should be important to consider when analyzing extreme wave events but also when analyzing extreme water level events even if fewer locations are concerned for the wave setup scaling.

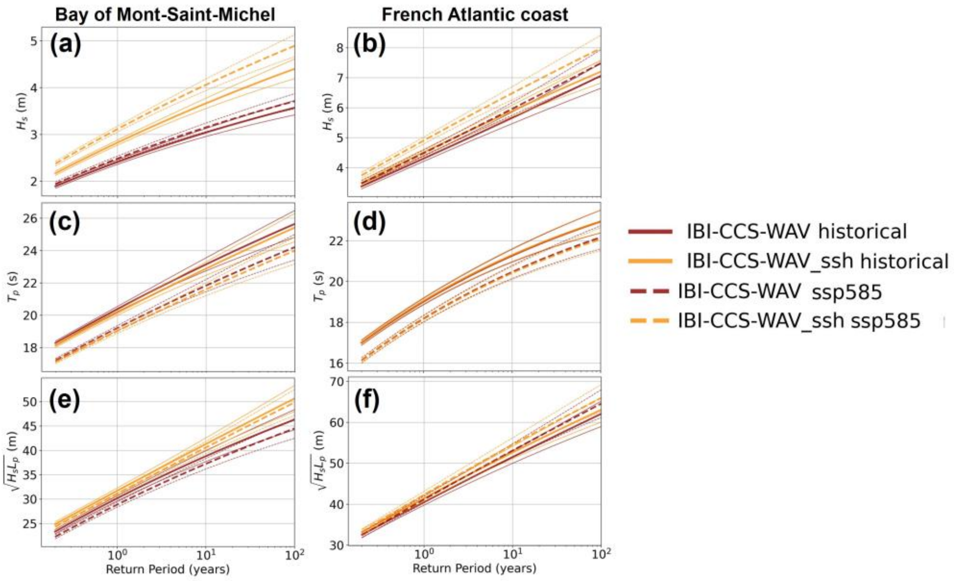

Figure 14: Return period curves of incomingsignificant wave conditionsheight (H_s, in m) for IBI-CCS-WAV (dark red curves) and IBI-CCS-WAV_ssh (dark yellow curves) for (a) the Bay of Mont-Saint-Michel (first column) and for(b) the French Atlantic coast (second column) (Fig. 2b1b). The solid lines represent the year 1985 (representative of the 1970-2000-2006 period) and the dashed lines the year 2085 (representative of the 20702081-2100 period) for under the SSP5-8.5 scenario. The rows show 3 variables: (a,b) significant wave height (Hs, in m), (c,d) peak period (Tp, in s) and (e,f) scaling for wave setup ($\sqrt{H_sL_p}$, in m). The thin solid and dashed lines are the confidence intervals (corresponding to 1 sigma confidence)

Mis en forme : Police :10 pt, Couleur de police : Automatique

Mis en forme : Police :+Corps (Times New Roman), Gras, Couleur de police : Automatique

Mis en forme : Police :10 pt, Couleur de police : Automatique

Mis en forme : Police :10 pt, Couleur de police : Automatique

Mis en forme : Police :10 pt, Couleur de police : Automatique

Mis en forme : Police :10 pt, Couleur de police : Automatique

Mis en forme : Police :10 pt, Couleur de police : Automatique

Mis en forme : Police :10 pt, Couleur de police : Automatique

Mis en forme : Police :10 pt, Couleur de police : Automatique

Mis en forme : Police :10 pt, Couleur de police : Automatique

Mis en forme : Police :10 pt, Couleur de police : Automatique

Mis en forme : Police :10 pt, Couleur de police : Automatique

Mis en forme : Police :10 pt, Couleur de police : Automatique

Mis en forme : Police :10 pt, Couleur de police : Automatique

Mis en forme : Police :10 pt, Couleur de police : Automatique

Mis en forme : Police :10 pt, Couleur de police : Automatique

associated with the extreme value analysis (EVA). The differences between IBI-CCS-WAV and IBI-CCS-WAV_ssh are considered significant when the confidence intervals associated with the return levels calculation are disjoint.

The return period curves for the Bay of Mont-Saint-Michel and for the French Atlantic coast are displayed in Figure 14 for the two simulations IBI-CCS-WAV and IBI-CCS-WAV_ssh. In the Bay of Mont-Saint-Michel, the differences between the two simulations are very important for the 1970-2000 period (dark curves) for the significant wave height (Fig. 14a). It is especially the case for high return periods such as the 100-year return level. As the confidence intervals for the two simulations are disjoint, the differences are considered significant. For the 2070-2100 period under the SSP5-8.5 scenario, the differences between the two simulations are even larger due to the mean sea level rise of about +80 cm. For example, in the case of the significant wave height, the 100-year return level is +35 % larger when considering the water level variations and for the wave setup scaling it represents an increase of +11 %. In terms of wave setup, using parameterization (1), the differences in the wave setup can reach from +7 cm to +12.25 cm for the 100-year return level depending on the beach slope. This value seems small but is important to consider in the context of threshold exceedance calculations to predict coastal flooding. For the French Atlantic coast, the confidence intervals between IBI-CCS-WAV and IBI-CCS-WAV_ssh are not distinct. Therefore, the differences due to the inclusion of the water level variations on the wave model are not considered significant. Overall, the longer the return periods, the larger the differences between the two simulations.

To better assess the impact of sea level variations on the extreme significant wave heights, return period curves are displayed in Figure 11 for the two locations. The higher the return periods, the larger the impact of the non-linear interaction of sea level on waves. For instance, in the Bay of Mont-Saint-Michel, the 1-in-100-year return level of significant wave height is +60 % larger when considering sea level variations in the wave model (Fig. 11a). At the end of the century, the differences between the two simulations are even larger and can reach +70 % mainly due to the mean sea level rise of about +80 cm under the SSP5-8.5 scenario. The curves also indicate that considering the interaction of sea level on waves modifies the shape of the return period curve, which may have important implications for the future amplifications of extreme events.

5 Discussion

5.1 Model resolution limitations

The use of a single forcing climate model does not allow to quantify the uncertainties of the projected changes. Here, the focus of the study is not providing a likely range of wave projected changes over the IBI domain but rather the focus is process-oriented. In our study, the estimation of the impact of including the hourly watersea level variations in the wave model is limited by several resolution aspects. The first limitation is the horizontal resolution of the wave model. The model resolution of 1/10 ° (~10 km) is conditioned by the computational cost due to the length of the simulations needed to address the question of extremes in aon climate sealescales. It does not allow a very fine representation of the coastline and of the bathymetry in the coastal zones. For instance, to maintain a realistic balance betweenMoreover, the 10 km horizontal resolutionregional ocean model (Tab. 1 and Appendix A) used for the water depth, the minimumsurface currents and sea level forcing does not allow for dry areas. Therefore, a minimal bathymetry is set to 6 m (i.e. time-mean minimum of to run the ocean model with tides (Chaigneau et al. 2022). We chose to apply the same minimal bathymetry of 6 m) in the regional wave model to maintain consistency between both regional ocean and wave models. In fact, because it would have been unrealistic to have a bathymetry of 1 m within a 10 km grid point. In consequence, the wave model has , the minimum bathymetry (6 m) also allows to maintain a realistic balance between the 10 km horizontal resolution and the water depth. This results in fewer areas of shallow and intermediate and shallow water areas than a higher resolutionin the wave model and thus less non-linear interactions.effect of sea level variations on the waves. The implementation of "wetting and drying" (O'Dea et al., 2020) allowing for dry areas in NEMO version 4.2 should improve this limitation on the ocean model and therefore on the wave model. Another limitation that may limit the non-linear interactions between waves and water level is the resolution of the atmospheric forcing from the global climate model (Sect. 2.3.2Tab. 1). Given that winds are the major drivers of extreme wave events in our study, the relative coarseeven with a relatively high-resolution climate model forcing, the resolution of 50 km for the atmospheric drivers (~50 km) implies that generated waves are more representative of a large-scale forcing than of coastal processes. Therefore, the results

For all these reasons, the estimates provided in this study only partially represent the processes responsible for the non-linear interaction of sea level on waves and the results found in this study are not representative of the realany purely local situation at the coast but rather give aprovide regional information. A second step of dynamical downscaling at higher resolution would be necessary to overcome such resolution limitations.

5.2 Limitations associated with the use of parametrizations for the wave setup

Limitations in the use of parametrizations to estimate wave setup are thoroughly discussed in Melet et al., 2020; Lambert et al., 2020, including sensitivity analyses of the wave setup and runup contributions to different empirical parametrizations. The generic parametrization of Stockdon et al., 2006 used to compute the wave setup in our study is indeed subject to intrinsic limitations. A major limitation is that the formulation is only representative of sandy beaches. Other parameterizations (Guza and Thornton, 1981; Holman, 1986; dissipative case of Stockdon et al., 2006 or for a review Dodet et al. 2019) exist but they

Mis en forme : Couleur de police : Automatique
Mis en forme : Couleur de police : Noir
Mis en forme : Couleur de police : Automatique
Mis en forme : Couleur de police : Automatique
Mis en forme : Couleur de police : Automatique
Mis en forme : Couleur de police : Automatique
Mis en forme : Couleur de police : Automatique
Mis en forme : Couleur de police : Automatique
Mis en forme : Couleur de police : Automatique
Mis en forme : Couleur de police : Automatique
Mis en forme : Couleur de police : Automatique, Anglais (États-Unis)
Mis en forme : Couleur de police : Automatique, Anglais (États-Unis)
Mis en forme : Couleur de police : Automatique, Anglais (États-Unis)
Mis en forme : Couleur de police : Automatique, Anglais (États-Unis)
Mis en forme : Couleur de police : Automatique, Anglais (États-Unis)
Mis en forme : Couleur de police : Automatique, Anglais (États-Unis)
Mis en forme : Couleur de police : Automatique
Mis en forme : Couleur de police : Automatique
Mis en forme : Couleur de police : Automatique
Mis en forme : Couleur de police : Automatique
Mis en forme : Couleur de police : Automatique
Mis en forme : Couleur de police : Automatique
Mis en forme : Couleur de police : Automatique
Mis en forme : Couleur de police : Automatique
Mis en forme : Couleur de police : Automatique
Mis en forme : Couleur de police : Automatique
Mis en forme : Couleur de police : Automatique
Mis en forme : Couleur de police : Automatique
Mis en forme : Couleur de police : Automatique
Mis en forme : Couleur de police : Automatique
Mis en forme : Couleur de police : Automatique

are often limited to specific coastal environments (e.g. dissipative sandy beaches, rocky cliffs) and have been calibrated with relatively few field data. The calibration therefore does not cover all the spectra of the environmental conditions.

For our large-scale study, another major limitation is that the parameterization relies on the specification of a beach slope. As explained in Melet et al., 2020, the beach slope evolves over different time scales (extreme events, seasonal, interannual, and in response to sea level rise) and spatial scales (from alongshore at a given local beach to regional scales) and generally ranges between 0.01 and 0.20 (Komar, 1998). At the moment, however, no observations of the foreshore beach slope applicable in empirical formulations is available worldwide or in Europe. Therefore, a time and space constant beach slope value is commonly used for global and regional studies (Serafin et al., 2017; Melet et al., 2018, 2020a), as done in this study. In Melet al., 2020, a beach slope of 0.04 is used, corresponding to the median value of local values at 308 sites along the global ocean coastlines. In Serafin et al., 2017, a constant beach slope of 0.05 is used corresponding to the regional mean based on observations for the west coast of USA. In Vos et al., 2020, regional beach slopes are provided for the coasts of southeastern Australia and USA California based on satellite data. The spatial mean of these regional estimates is 0.06±0.02 for the Australia and 0.07±0.02 for California. All these values for β are in the tested range of 0.04-0.07.

5.3 Limitations associated with the applicability of the parametrization to coastal points

To calculate the wave setup for the coastal points of our regional domain, we chose to use the simple parameterization of Stockdon et al., 2006 based on deep water parameters. However, the coastal points are theoretically not purely deep water as shown in Figure 2a (yellow dotted lines). Yet, this approach, used in other climate studies (Melet et al., 2018, 2020a; Lambert et al., 2020), appears pragmatic given the model resolution limitations (Sect. 5.1) and the processes accounted for in the wave model (Sect. 2.1).

5.4 Impact of the absence of depth-induced wave breaking

Very close to the coast, the depth-induced wave breaking is a fundamental depth-dependent process that can have a first-order effect on the shallow water wave statistics and thus on the wave setup. As explained in Sect. 2.1, the physics associated with the explicit representation of coastal breaking waves is not activated. Such an approach is justified because our primary interest is to calculate the wave setup contribution to include it in further analyses on extreme water levels and the parameterization used to compute this contribution is based on deep water parameters (Sect. 2.5) that are not supposed to be affected by coastal wave breaking. In consequence, as the regional wave model does not have a very fine representation of the bathymetry or the coastline (Sect. 5.1) and does not resolve the wave transformations in the coastal zones, the estimates provided in this study only partially represent the processes responsible for the wave-water level non-linear interactions.

With the coastal wave breaking included, the significant wave heights should be substantially impacted in shallow waters. The impact of the inclusion of the water level variations in the wave model would also probably differ. A perspective for this study would be to take into account coastal wave breaking and to apply new specific wave setup formulations which would not require deep water characteristics or to use a wave model that directly resolve the wave setup.

5.55.2 Impact of waves on sea level

The aim of the study was to better understand the non-linear interactions between waves and sea level. In the modeling framework of the paper, only the effect of sea level on waves is accounted for. However, both are coupled in reality with waves impacting on sea level. For instance, Bonaduce et al., 2020 have studied the contribution of wave processes to sea level variability over the European Seas with ocean-wave coupled simulations at an eddy-resolving spatial resolution of 3.5 km. They highlighted the occurrence of mesoscale features of the ocean circulation and a modulation of the surge at the shelf break due to the effect of the wave forcing on sea level. More importantly, they also reported a large contribution of wave induced processes to sea level extremes which are up to 20 % higher on the European continental shelf due to these wave processes. By consideringtaking these processes into account in the ocean model, as the watersea level would be higher, the impact on the wave model would be larger which means increased wave-water, meaning an increase in waves-sea level feedbacks.

5.63 Implications of the results for coastal flooding

The results obtained in this study have shown a large impact of sea level variations on extreme significant wave projectionsheights. Wind-waves and swell contribute to extreme sea levels at the coast via wave setup and runup (Dodet et al., 2019), combined with tides, storm surges and mean sea level changes. Marine flooding hazards cannot be quantified based on wave contributions alone but these contributions can locally partially enhance sea level changes at the coast (Melet et al., 2020a). Our results show that extreme significant wave heights are strongly influenced by the effect of sea level on waves in coastal areas subject to large sea level variations or on wide continental shelves. Depending on the region (wave regimes, sign of the extreme wave projected changes, local ocean processes involved, amplitude of projected changes in local sea level), the impact of the sea level changes on waves could be important to consider for present and future flooding hazards (e.g. for threshold exceedance calculations). For instance, future waves conditions and therefore coastal flooding could be affected in areas where large changes in tides are projected such as in the China Sea and Gulf of Saint Lawrence (Pickering et al., 2017, Haigh et al., 2019). Future extreme waves could also be significantly impacted in areas subject to large relative mean sea level

Mis en forme : Couleur de police : Automatique

Mis en forme : Couleur de police : Automatique

Mis en forme : Couleur de police : Automatique

Mis en forme : Couleur de police : Automatique

Mis en forme : Couleur de police : Automatique

Mis en forme : Couleur de police : Automatique

Mis en forme : Couleur de police : Automatique, Anglais (États-Unis)

Mis en forme : Couleur de police : Automatique

Mis en forme : Couleur de police : Bleu

Mis en forme : Couleur de police : Automatique

Mis en forme : Couleur de police : Automatique

Mis en forme : Normal, Espace Avant : 12 pt, Après : 12 pt

Mis en forme : Couleur de police : Automatique

Mis en forme : Couleur de police : Automatique

rise, such as along the eastern coasts of the United States, the Gulf of Mexico and the Caribbean Sea where a rise of +1.4 m is expected by the end of the century under the SSP5-8.5 scenario (Fox-Kemper et al., 2021).

~~Marine flooding hazards cannot be quantified based on wave setup alone but wave setup can locally partially balance or enhance water levels at the coast (Melet et al., 2020a). Depending on the location (wave regimes, local ocean processes involved, sign of the extreme wave projected changes, amplitude of the projected changes in ocean processes), the inclusion of the non-linear interactions could thus enhance or balance the future wave extremes and may be important to consider for future flooding hazard calculations. The results presented in this study highlight that wave-water level non-linear interactions can be substantial for extreme wave height and wave setup, but are region dependent. For instance, the extreme wave projections are directly dependent on the water level variations forcing. In our case, the future water level variations and therefore a large part of the non-linear interactions are mainly associated with the mean sea level rise of about +80 cm and less so to changes in tides or storm surges. In other regions, large projected changes in tides or storm surges could impact the future waves conditions. For instance, Pickering et al., 2017 and Haigh et al., 2019 showed changes up to + 20 cm in the M2 component in the China Sea and in the Gulf of Saint Lawrence. Then, the future wave extremes could also be substantially more impacted in areas subject to larger mean sea level rise such as along the eastern coasts of the United States, in the Gulf of Mexico and in the Caribbean Sea where a rise of +1.4 m is expected at the end of the century under scenario SSP5-8.5 (Fox-Kemper et al., 2021).~~

6 Conclusions

Several studies have shown that water depth changes~~ induced by sea level rise~~ can induce changes in the wave field at a fine spatial scale (Hoeke et al., 2015; Arns et al., 2017; Lewis et al., 2019; Idier et al., 2019; Calvino et al., 2022). The aim of ~~the present~~this paper was to characterize, at a larger scale, the sensitivity of historical and projected sea states to the non-linear ~~interactions between waves and water~~interaction of sea level ~~changes~~ (tides, storm surge, mean sea level ~~rise),~~changes) on waves, notably during extreme events. To address this question, a regional wave model has been adapted to include ~~the wave-water~~sea level ~~interactions~~variations over the northeastern Atlantic for the ~~1950~~1970-2100 period. This is one of the first studies assessing the impact of sea level changes on waves conditions at such a regional large-scale.

~~As a first step~~First, the regional wave model ~~has been~~is presented and validated over the 1993-2014 period. Comparisons to observations and a wave reanalysis ~~showed~~show an overall good performance of the model. Secondly, as we used a single forcing climate model, projected regional changes in mean and extreme wave conditions ~~were~~are compared to previous studies. They ~~were~~are shown to be representative of other published projections over the northeastern Atlantic region, with a general decrease in mean and extreme significant wave height and peak period under the SSP5-8.5 scenario.

The impact of including hourly ~~water~~sea level variations in the wave model ~~was~~is assessed over the historical period and for 21^{st} century projections for the mean state and extremes of wind-wave characteristics~~ and wave setup, the latter contributing to coastal sea level hazards such as coastal flooding. For the historical period, wave-water level interactions .~~. The impact on the mean ~~wave~~ state ~~and wave setup were~~ is found to be ~~small. The impact of water level changes on wave conditions~~weak in general over the historical period ~~is substantially more important when considering the 99^{th} percentile or 100-year return level along the coasts of the large continental shelf and particularly in large tidal range areas. For example, in the Bay of Mont-Saint-Michel where the tidal range is of 10 meters, extreme significant wave heights were found to be larger by 1 meter (or +25 %) during a historical extreme wave event when considering hourly water level variations in the wave model. The corresponding increase in wave setup reached +8.4 cm and +14.7 cm, when considering beach slopes of 4 % and 7 % respectively. However, these values are the upper bound of the sensitivity of significant wave height and wave setup to wave-water level interactions with the settings of our model, as the Bay of Mont-Saint-Michel is subject to one of the largest tidal ranges of the IBI domain.~~

~~Mean~~and at the end of the 21^{st} century. Over the northeastern Atlantic, mean sea level rise and, to a lesser extent, changes in tidal amplitudes and storm surges reach approximately +80 cm in 2100 compared to the 1986-2005 ~~mean under~~period for the SSP5-8.5 ~~high-emission climate change~~ scenario~~ over the northeastern Atlantic (Chaigneau et al. 2022).~~. This increase leads to mean ~~sea level rise has an overall effect in our regional projections of the mean wave state over the large continental shelf where shallow and intermediate water dynamics prevail. Significant wave heights are projected to be~~ significant wave heights up to +3 cm (or +6 %) higher along the French Atlantic coasts and in the southern North Sea by the end of the 21^{st} century~~ due to water depth changes.~~. The impact of ~~accounting for wave-water level interactions on the wave setup mean state is of the same order of magnitude (+6 %). However, it should be noted that these impacts are found in locations where projected changes in significant wave height over the 21st century are generally small since the largest projected changes are located in the southern part of the regional domain. The main impact of the inclusion of hourly water level variations in the wave model is found during extreme events (99^{th} percentile or 100-year return level) at the end of the 21^{st} century. For high return period events, the consideration in the wave model of~~sea level variations is substantially more important on extreme significant wave heights over the wide continental shelf where shallow water dynamics prevail and particularly in large tidal range areas. For example, in the Bay of Mont-Saint-Michel where the tidal range is of 10 m, extreme significant wave heights are found to be larger by 1 m (or +30 %) during a historical extreme wave. Accounting for the combination of tides, storm surges and sea level rise in the wave model also lead to ~~greater~~higher values of 1-in~~ extreme~~-100-year significant wave ~~height by~~heights, up to +20

Mis en forme : Couleur de police : Automatique, Anglais (États-Unis)

Mis en forme : Couleur de police : Noir

Mis en forme : Couleur de police : Automatique (×33)

Mis en forme : Couleur de police : Couleur personnalisée(RVB(28;29;30))

~~% for many locations~~40 % at the end of the 21st century~~. The impact on~~ located in the ~~wave setup can be up to +10 % but fewer locations are concerned. Overall~~Bay of Biscay, the ~~inclusion of water level variations on the wave model had almost no impact on the peak period.~~

~~However~~North Sea, around United Kingdom and Ireland. Moreover, as the regional wave model does not have a very fine representation of the bathymetry~~ or~~, of the coastline and does not ~~resolve the depth-induced wave breaking in the shallow areas~~include the feedback of waves on sea level, the estimates provided in this study only partially represent the processes responsible for the ~~wave-water~~sea level-wave non-linear interactions. ~~Moreover~~Overall, the ~~results found might be dependent~~inclusion of water level variations on the ~~parametrization used to compute the~~ wave ~~setup and therefore~~model had almost no impact on the ~~beach slopes.~~peak period.

In conclusion, our results advocate for the inclusion of ~~wave-water~~sea level-wave non-linear interactions in ~~modelling~~modeling studies of wave extremes at this resolution or higher, in particular when extreme significant wave heights are of interest. These non-linear interactions should be accounted for when threshold exceedances are calculated for example in order to prevent coastal flooding or to build coastal protection structures in a climate change context.

Code availability

The MFWAM model used in this study is based on the wave model WAM freely available at https://github.com/mywave/WAM.

Data availability

Information on CNRM-CM6- 1-HR simulations can be found at https://doi.org/10.22033/ESGF/CMIP6.4067 (CNRM-CM6-1-HR, historical; Voldoire, 2019a), https://doi.org/10.22033/ESGF/CMIP6.4164 (CNRM-CM6-1-HR, piControl; Voldoire, 2019b), https://doi.org/10.22033/ESGF/CMIP6.~~4185 (CNRM-CM6-1-HR, ssp126; Voldoire, 2020a), https://doi.org/10.22033/ESGF/CMIP6.~~4225 (CNRM-CM6-1-HR, ssp585; Voldoire, 2019c). The CNRM-CM6-1-HR forcing fields are available on the ESGF website (ESGF, 2022a: historical data, http://esgf-data.dkrz.de/search/cmip6-dkrz/?mip_era=CMIP6&activity_id=CMIP&institution_id=CNRM-CERFACS&source_id=CNRM-CM6-1-HR&experiment_id=historical; ESGF, 2022b: piControl data, http://esgf-data.dkrz.de/search/cmip6-dkrz/?mip_era=CMIP6&activity_id=CMIP&institution_id=CNRM-CERFACS&source_id=CNRM-CM6-1-HR&experiment_id=piControl; ESGF, 2022c: ~~ssp126 data, http://esgf-data.dkrz.de/search/cmip6-dkrz/?mip_era=CMIP6&activity_id=ScenarioMIP&institution_id=CNRM-CERFACS&source_id=CNRM-CM6-1-HR&experiment_id=ssp126; ESGF, 2022d:~~ ssp585 data, http://esgf-data.dkrz.de/search/cmip6-dkrz/?mip_era=CMIP6&activity_id=ScenarioMIP&institution_id=CNRM-CERFACS&source_id=CNRM-CM6-1-HR&experiment_ id=ssp585). The reanalysis data and wave buoy observations were obtained from the Copernicus Marine Services (Copernicus, 2022a: reanalysis data, https://doi.org/10.48670/moi-00030; Copernicus, 2022b: observational data, https://doi.org/10.13155/53381).

Author contribution:

AM designed the study. LA prepared the regional wave model configuration. SLC adapted the regional wave model to consider hourly variations of sea level and performed the regional wave simulations. AAC performed the sea level regional simulations and did the analyses of the study. AM, AV, GR, SLC and LA supervised the project. AM and AAC wrote the introduction, ~~SLC~~AAC wrote the Methods~~ section and AAC wrote the~~, Results, Discussion and Conclusions sections. All authors contributed to manuscript revisions and read and approved the submitted version.

Competing interests:

All authors declare that they have no conflicts of interest.

Acknowledgements

Analyses were carried out with Python. The authors thank Joanna Staneva for her advice and help on the implementation of the sea level forcing in the regional wave model.

Financial support

The PhD thesis of AAC is supported by Mercator Ocean and Météo-France.

Mis en forme : Couleur de police : Automatique

Mis en forme : Couleur de police : Automatique

Mis en forme : Couleur de police : Automatique

Mis en forme : Couleur de police : Automatique

Mis en forme : Couleur de police : Automatique

Mis en forme : Couleur de police : Automatique

Mis en forme : Couleur de police : Automatique

Mis en forme : Couleur de police : Automatique

Mis en forme : Couleur de police : Automatique, Anglais (États-Unis)

Mis en forme : Couleur de police : Automatique

Mis en forme : Couleur de police : Automatique, Non Surlignage

Mis en forme : Couleur de police : Automatique, Non Surlignage

Mis en forme : Couleur de police : Automatique, Non Surlignage

Mis en forme : Couleur de police : Automatique, Anglais (États-Unis)

Mis en forme : Couleur de police : Automatique

Mis en forme : Couleur de police : Automatique

Mis en forme : Couleur de police : Automatique

Mis en forme : Couleur de police : Automatique

Mis en forme : Couleur de police : Automatique

Mis en forme : Couleur de police : Automatique

Mis en forme : Couleur de police : Automatique

Mis en forme : Couleur de police : Automatique

Mis en forme : Couleur de police : Automatique

Mis en forme : Couleur de police : Automatique

Appendix A : External forcings used to produce the regional wave simulations

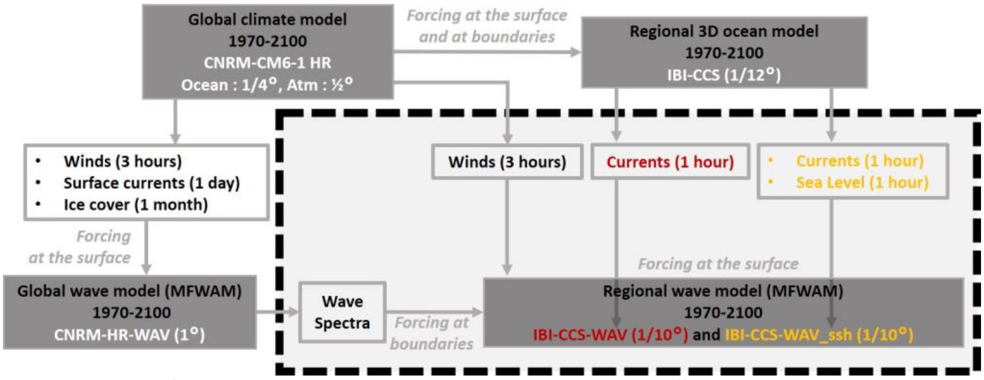

Figure A1: Sketch of the downscaling strategy explaining the links between the different simulations used in this study.

1 Wave forcing from CNRM-HR-WAV global wave simulations

The regional wave simulations IBI-CCS-WAV and IBI-CCS-WAV_ssh described in Sect. 2.2 and Sect. 2.3 are forced at lateral boundaries by 3-hourly wave spectra information from CNRM-HR-WAV global wave simulations (Fig. A1, Tab. 1). CNRM-HR-WAV simulations are produced over the 1970-2100 period using the MFWAM wave model (Sect. 2.1) at a 1 ° resolution. These simulations are forced by 3-hourly surface winds (1/2 °), monthly sea-ice cover (1/4 °) and daily ocean surface currents (1/4 °) taken from the CMIP6 CNRM-CM6-1-HR global climate simulations (Voldoire et al., 2019; Saint-Martin et al., 2021). The historical simulation of CNRM-CM6-1-HR is used over the 1970-2014 period. Then, over the 2015-2100 period, the SSP5-8.5 climate change scenario simulations is used (O'Neill et al., 2016).

CNRM-HR-WAV simulations use 2-min gridded global topography data from ETOPO2/NOAA (National Geophysical Data Center 2006). The model grid has a constant spacing in longitude but is compressed in latitude to maintain a constant resolution (Bidlot, 2012). A wave growth calibration was performed to adjust the mean significant wave height of CNRM-HR-WAV to the Copernicus Marine Service WAVERYS wave reanalysis (Law-Chune et al., 2021) over the IBI domain. The wave spectrum is discretized in 24 directions and 30 frequencies starting from 0.035 up to 0.58 Hz. Classical integrated wave parameters such as significant wave height (H_S) or peak period (T_p) are output at a three-hourly from CNRM-HR-WAV.

2 Atmospheric forcing from CNRM-CM6-1-HR global climate model

Regional wave projections are driven by the same 3-hourly surface winds as CNRM-HR-WAV (Sect. A1.1) produced by the CNRM-CM6-1-HR global climate model (Voldoire et al., 2019; Saint-Martin et al., 2021), which is part of the CMIP6 database. The use of a global climate model with a higher spatial resolution compared to the typical coarse resolutions of CMIP5 and 6 models was interesting for the atmosphere (1/2 °) for the intensity of the winds notably.

By driving our simulations with only one global climate model simulation, the aim of the study was not to characterize the uncertainties of wave projected changes over the IBI domain, but rather to discuss the impact of the sea level changes on the downscaled projections. However, before using the winds to force the global and regional wave models, we verified that CNRM-CM6-1-HR was consistent with other CMIP6 global climate models in particular in terms of extreme winds and their projections. A comparison of extreme winds (99th percentile) between CNRM-CM6-1-HR, some other CMIP6 global climate models, the atmospheric reanalysis ERA5 (Hersbach et al., 2020) and wind observations from wave buoys (Wehde et al., 2021) is performed at different locations in the IBI region (Fig. A2a). The three different locations considered (shown in Fig. 1) are chosen along storm trajectories in the northeastern Atlantic and North Sea (Lozano et al., 2004). Figure A2a shows that CNRM-CM6-1-HR is representative of an ensemble of 21 CMIP6 models over the historical period. In general, CNRM-CM6-1-HR also agree with ERA5 which is the reference here. However, wave buoys observations seem to be significantly different from

Mis en forme : Couleur de police : Automatique
Mis en forme : Couleur de police : Bleu
Mis en forme : Couleur de police : Automatique
Mis en forme : Couleur de police : Automatique
Mis en forme : Couleur de police : Automatique
Mis en forme : Couleur de police : Automatique

both the global climate models and ERA5, except in the North Sea. Figure A2b shows the projected changes for the extreme wind speed at the three locations. Projected changes in extreme wind speed are quite small in all models and rather uncertain (large interquartile range). Projected changes are of the same sign for 7, 9 and 10 models out of twelve for the three boxes respectively. In the English Channel and North Sea, CNRM-CM6-1-HR shows an increase in extreme wind speed which is representative of the other CMIP6 models. In the North Atlantic, CNRM-CM6-1-HR exhibits a large decrease in extreme wind speed which is in the high range (in absolute value) of CMIP6 models but still of the same sign as most models.

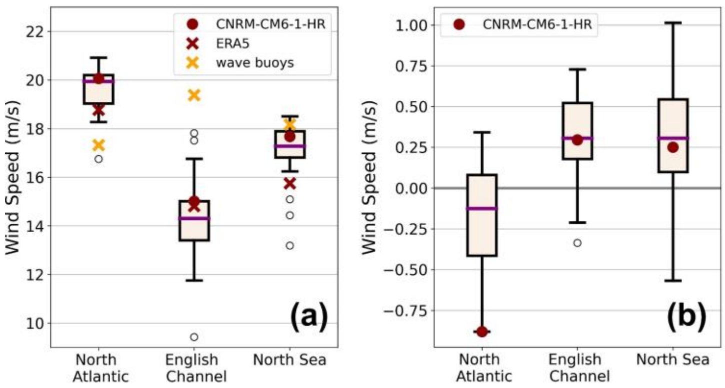

Figure A2: (a) Extreme winds (99th percentile) for CNRM-CM6-1-HR (dark red dot), 21 different CMIP6 global climate models (black box), the atmospheric reanalysis ERA5 (dark red cross) and wind observations from wave buoys (yellow cross) at the three locations in the IBI region marked on Fig. 2a for the 1993-2014 period. The 2011-2022 period was chosen for the wave buoy in the North Sea as it was the only period available. (b) Projected changes in extreme wind speed for CNRM-CM6-1-HR and 12 different CMIP6 climate models at the three locations marked on Fig. 2a under the SSP5-8.5 scenario (2081-2100 vs 1986-2005). The selected CMIP6 climate models are those with three-hourly atmospheric outputs. In (a) and (b), the purple line represents the median, the black box represents the interquartile range and the whiskers represent the last model under or above 1.5 times the interquartile range. The black circles represent the outlier models i.e. models outside 1.5 times the interquartile range. Units are in m s^{-1}.

3 Ocean forcing from IBI-CCS regional ocean model

IBI-CCS-WAV regional wave projections are also forced by hourly surface current (and hourly sea level variations in the dedicated simulation IBI-CCS-WAV_ssh) of IBI-CCS, a 3D regional ocean model at a 1/12 ° horizontal resolution, itself forced by CNRM-CM6-1-HR global climate model. IBI-CCS was implemented in Chaigneau et al., 2022 to refine sea level projections of CNRM-CM6-1-HR over the northeastern Atlantic region through a dynamical downscaling. For a more complete representation of processes driving coastal sea level changes, tides and atmospheric surface pressure forcing are explicitly resolved in IBI-CCS in addition to the mean sea level (including ocean general circulation (dynamic sea level)).

References

Aarnes, O. J., Reistad, M., Breivik, Ø., Bitner-Gregersen, E., Ingolf Eide, L., Gramstad, O., Magnusson, A. K., Natvig, B., and Vanem, E.: Projected changes in significant wave height toward the end of the 21st century: Northeast Atlantic: PROJECTED CHANGES IN WAVE HEIGHT, J. Geophys. Res. Oceans, 122, 3394–3403, https://doi.org/10.1002/2016JC012521, 2017.

Alari, V.: Multi-Scale Wind Wave Modeling in the Baltic Sea, 2013.

Almar, R., Ranasinghe, R., Bergsma, E. W. J., Diaz, H., Melet, A., Papa, F., Vousdoukas, M., Athanasiou, P., Dada, O., Almeida, L. P., and Kestenare, E.: A global analysis of extreme coastal water levels with implications for potential coastal overtopping, Nat Commun, 12, 3775, https://doi.org/10.1038/s41467-021-24008-9, 2021.

Aouf, L. and Lefèvre, J.-M.: On the Impact of the Assimilation of SARAL/AltiKa Wave Data in the Operational Wave Model MFWAM, Marine Geodesy, 38, 381–395, https://doi.org/10.1080/01490419.2014.1001050, 2015.

Ardhuin, F., ~~Rogers, E., Babanin, A. V., Filipot, J. F., Magne, R., Roland, A., Westhuysen, A. van der, Queffeulou, P., Lefevre, J.-M., Aouf, L., and Collard, F.: Semiempirical Dissipation Source Functions for Ocean Waves. Part I: Definition, Calibration, and Validation, Journal of Physical Oceanography, 40, 1917–1941, https://doi.org/10.1175/2010JPO4324.1, 2010.~~

Ardhuin, F., Roland, A., Dumas, F., Bennis, A.-C., Sentchev, A., Forget, P., Wolf, J., Girard, F., Osuna, P., and Benoit, M.: Numerical Wave Modeling in Conditions with Strong Currents: Dissipation, Refraction, and Relative Wind, Journal of Physical Oceanography, 42, 2101–2120, https://doi.org/10.1175/JPO-D-11-0220.1, 2012.

Arns, A., Dangendorf, S., Jensen, J., Talke, S., Bender, J., and Pattiaratchi, C.: Sea-level rise induced amplification of coastal protection design heights, Sci Rep, 7, 40171, https://doi.org/10.1038/srep40171, 2017.

Battjes, J. A. and Janssen, J. P. F. M.: Energy loss and set-up due to breaking random waves, Proceedings of 16th Conference on Coastal Engineering, Hamburg, Germany, 1978, 1978.

Bergsma, E. W. J., Almar, R., Anthony, E. J., Garlan, T., and Kestenare, E.: Wave variability along the world's continental shelves and coasts: Monitoring opportunities from satellite Earth observation, Advances in Space Research, 69, 3236–3244, https://doi.org/10.1016/j.asr.2022.02.047, 2022.

Bidlot, J., Janssen, P., and Abdalla, S.: A revised formulation of ocean wave dissipation and its model impact, 27, 2007.

Bidlot, J.: Present status of wave forecasting at ECMWF. In: Workshop on Ocean Waves. ECMWF, Reading, United Kingdom, 2012.

Bonaduce, A., Staneva, J., Grayek, S., Bidlot, J.-R., and Breivik, Ø.: Sea-state contributions to sea-level variability in the European Seas, Ocean Dynamics, 70, 1547–1569, https://doi.org/10.1007/s10236-020-01404-1, 2020.

Bruciaferri, D., Tonani, M., Lewis, H. W., Siddorn, J. R., Saulter, A., Castillo Sanchez, J. M., Valiente, N. G., Conley, D., Sykes, P., Ascione, I., and McConnell, N.: The Impact of Ocean-Wave Coupling on the Upper Ocean Circulation During Storm Events, Journal of Geophysical Research: Oceans, 126, e2021JC017343, https://doi.org/10.1029/2021JC017343, 2021.

Calvino, C., Dabrowski, T., and Dias, F.: A study of the wave effects on the current circulation in Galway Bay, using the numerical model COAWST, Coastal Engineering, 180, 104251, https://doi.org/10.1016/j.coastaleng.2022.104251, 2022.

Carvalho, D., Rocha, A., Costoya, X., deCastro, M., and Gómez-Gesteira, M.: Wind energy resource over Europe under CMIP6 future climate projections: What changes from CMIP5 to CMIP6, Renewable and Sustainable Energy Reviews, 151, 111594, https://doi.org/10.1016/j.rser.2021.111594, 2021.

Casas-Prat, M., Wang, X. L., and Swart, N.: CMIP5-based global wave climate projections including the entire Arctic Ocean, Ocean Modelling, 123, 66–85, https://doi.org/10.1016/j.ocemod.2017.12.003, 2018.

Chaigneau, A. A., Reffray, G., Voldoire, A., and Melet, A.: IBI-CCS: a regional high-resolution model to simulate sea level in western Europe, Geoscientific Model Development, 15, 2035–2062, https://doi.org/10.5194/gmd-15-2035-2022, 2022.

Chen, G., Chapron, B., Ezraty, R., and Vandemark, D.: A Global View of Swell and Wind Sea Climate in the Ocean by Satellite Altimeter and Scatterometer, Journal of Atmospheric and Oceanic Technology, 19, 1849–1859, https://doi.org/10.1175/1520-0426(2002)019<1849:AGVOSA>2.0.CO;2, 2002.

Chini, N., Stansby, P., Leake, J., Wolf, J., Roberts-Jones, J., and Lowe, J.: The impact of sea level rise and climate change on inshore wave climate: A case study for East Anglia (UK), Coastal Engineering, 57, 973–984, https://doi.org/10.1016/j.coastaleng.2010.05.009, 2010.

Dodet, G., Bertin, X., Bouchette, F., Gravelle, M., Testut, L., and Wöppelmann, G.: Characterization of Sea-level Variations Along the Metropolitan Coasts of France: Waves, Tides, Storm Surges and Long-term Changes, Journal of Coastal Research, 88, 10, https://doi.org/10.2112/SI88-003.1, 2019.

ECMWF: IFS Documentation CY40R1, ECMWF, https://doi.org/10.21957/f56vvey1x, 2014.

Elsayed, S. M. and Oumeraci, H.: Effect of beach slope and grain-stabilization on coastal sediment transport: An attempt to overcome the erosion overestimation by XBeach, Coastal Engineering, 121, 179–196, https://doi.org/10.1016/j.coastaleng.2016.12.009, 2017.

Fortunato, A. B., Oliveira, A., Rogeiro, J., Tavares da Costa, R., Gomes, J. L., Li, K., de Jesus, G., Freire, P., Rilo, A., Mendes, A., Rodrigues, M., and Azevedo, A.: Operational forecast framework applied to extreme sea levels at regional and local scales, Journal of Operational Oceanography, 10, 1–15, https://doi.org/10.1080/1755876X.2016.1255471, 2017.

Fox-Kemper, B., Hewitt, H.T., Xiao, C., Aðalgeirsdóttir, G., Drijfhout, S.S., Edwards, T.L., Golledge, N.R., Hemer, M., Kopp, R.E., Krinner, G., Mix, A., Notz, D., Nowicki, S., Nurhati, I.S., Ruiz, L., Sallée, J.-B., Slangen, A.B.A., and Yu, Y.: Ocean, Cryosphere and Sea Level Change. In Climate Change 2021: The Physical Science Basis. Contribution of Working Group I to the Sixth Assessment Report of the Intergovernmental Panel on Climate Change [MassonDelmotte, V., Zhai, P., Pirani, A., Connors, S.L., Péan, C., Berger, S., Caud, N., Chen, Y., Goldfarb, L., Gomis, M.I., Huang, M., Leitzell, K., Lonnoy, E., Matthews, J.B.R., Maycock, T.K., Waterfield, T., Yelekçi, O., Yu, R., and Zhou, B. (eds.)]. Cambridge University Press. In Press. 2021

García San Martín L., Barrera E., Toledano C., Amo A., Aouf L., Sotillo M.,: Product User Manual (CMEMS-IBI-PUM-005-006), available at: https://catalogue.marine.copernicus.eu/documents/PUM/CMEMS-IBI-PUM-005-006.pdf (last access: 16 December 2022), 2021

~~Guza, R. T. and Thornton, E. B.: Wave set-up on a natural beach, Journal of Geophysical Research: Oceans, 86, 4133–4137, https://doi.org/10.1029/JC086iC05p04133, 1981.~~

~~Haigh, I. D., Pickering, M. D., Green, J. A. M., Arbic, B. K., Arns, A., Dangendorf, S., Hill, D. F., Horsburgh, K., Howard, T., Idier, D., Jay, D. A., Jänicke, L., Lee, S. B., Müller, M., Schindelegger, M., Talke, S. A., Wilmes, S.-B., and Woodworth, P. L.: The Tides They Are A-Changin': A Comprehensive Review of Past and Future Nonastronomical Changes in Tides, Their Driving Mechanisms, and Future Implications, Reviews of Geophysics, 58, e2018RG000636, https://doi.org/10.1029/2018RG000636, 2019.~~

~~Hasselmann, S., Hasselmann, K., Allender, J. H., and Barnett, T. P.: Computations and parameterizations of the nonlinear energy transfer in a gravity-wave spectrum. Part II: Parameterizations of the nonlinear energy transfer for application in wave models, Journal of Physical Oceanography, 15, 1378–1391, https://doi.org/10.1175/1520-0485(1985)015<1378:CAPOTN>2.0.CO;2, 1985.~~

Hemer, M. A., Fan, Y., Mori, N., Semedo, A., and Wang, X. L.: Projected changes in wave climate from a multi-model ensemble, Nature Clim Change, 3, 471–476, https://doi.org/10.1038/nclimate1791, 2013.

Hersbach, H., Bell, B., Berrisford, P., Hirahara, S., Horányi, A., Muñoz-Sabater, J., Nicolas, J., Peubey, C., Radu, R., Schepers, D., Simmons, A., Soci, C., Abdalla, S., Abellan, X., Balsamo, G., Bechtold, P., Biavati, G., Bidlot, J., Bonavita, M., De Chiara, G., Dahlgren, P., Dee, D., Diamantakis, M., Dragani, R., Flemming, J., Forbes, R., Fuentes, M., Geer, A., Haimberger, L., Healy, S., Hogan, R. J., Hólm, E., Janisková, M., Keeley, S., Laloyaux, P., Lopez, P., Lupu, C., Radnoti, G., de Rosnay, P., Rozum, I., Vamborg, F., Villaume, S., and Thépaut, J.-N.: The ERA5 global reanalysis, Quarterly Journal of the Royal Meteorological Society, 146, 1999–2049, https://doi.org/10.1002/qj.3803, 2020.

Hoeke, R. K., McInnes, K. L., and O'Grady, J. G.: Wind and Wave Setup Contributions to Extreme Sea Levels at a Tropical High Island: A Stochastic Cyclone Simulation Study for Apia, Samoa, Journal of Marine Science and Engineering, 3, 1117–1135, https://doi.org/10.3390/jmse3031117, 2015.

~~Holman, R. A.: Extreme value statistics for wave run-up on a natural beach, Coastal Engineering, 9, 527–544, https://doi.org/10.1016/0378-3839(86)90002-5, 1986.~~

Idier, D., Bertin, X., Thompson, P., and Pickering, M. D.: Interactions Between Mean Sea Level, Tide, Surge, Waves and Flooding: Mechanisms and Contributions to Sea Level Variations at the Coast, Surv Geophys, 40, 1603–1630, https://doi.org/10.1007/s10712-019-09549-5, 2019.

~~Komar, P. D.: Beach processes and sedimentation, 2nd ed., Prentice Hall, Upper Saddle River, N.J, 544 pp., 1998.~~

~~Lambert, E., Rohmer, J., Cozannet, G. L., and Wal, R. S. W. van de: Adaptation time to magnified flood hazards underestimated when derived from tide gauge records, Environ. Res. Lett., 15, 074015, https://doi.org/10.1088/1748-9326/ab8336, 2020.~~

Law-Chune, S., Aouf, L., Dalphinet, A., Levier, B., Drillet, Y., and Drevillon, M.: WAVERYS: a CMEMS global wave reanalysis during the altimetry period, Ocean Dynamics, 71, 357–378, https://doi.org/10.1007/s10236-020-01433-w, 2021.

Le Cozannet, Goneri et al. (2022). "Cross-Chapter Box SLR: Sea level rise". In: Climate Change 2022: Impacts, Adaptation and Vulnerability. Working group II contribution to the sixth Assessment Report of the Intergovermental Panel on Climate Change.

Levier B., Lorente P., Reffray G., Sotillo M.: Quality Information Document (CMEMS-IBI-QUID-005-002), available at: https://catalogue.marine.copernicus.eu/documents/QUID/CMEMS-IBI-QUID-005-002.pdf last access: 16 December 2022), 2020

Lewis, M. J., Palmer, T., Hashemi, R., Robins, P., Saulter, A., Brown, J., Lewis, H., and Neill, S.: Wave-tide interaction modulates nearshore wave height, Ocean Dynamics, 69, 367–384, https://doi.org/10.1007/s10236-018-01245-z, 2019.

Lobeto, H., Menendez, M., and Losada, I. J.: Future behavior of wind wave extremes due to climate change, Sci Rep, 11, 7869, https://doi.org/10.1038/s41598-021-86524-4, 2021.

Longuet-Higgins, M. S. and Stewart, R. w.: Radiation stresses in water waves; a physical discussion, with applications, Deep Sea Research and Oceanographic Abstracts, 11, 529–562, https://doi.org/10.1016/0011-7471(64)90001-4, 1964.

Lozano, I., Devoy, R. J. N., May, W., and Andersen, U.: Storminess and vulnerability along the Atlantic coastlines of Europe: analysis of storm records and of a greenhouse gases induced climate scenario, Marine Geology, 210, 205–225, https://doi.org/10.1016/j.margeo.2004.05.026, 2004.

Masselink, G., Castelle, B., Scott, T., Dodet, G., Suanez, S., Jackson, D., and Floc'h, F.: Extreme wave activity during 2013/2014 winter and morphological impacts along the Atlantic coast of Europe, Geophysical Research Letters, 43, 2135–2143, https://doi.org/10.1002/2015GL067492, 2016.

McMichael, C., Dasgupta, S., Ayeb-Karlsson, S., and Kelman, I.: A review of estimating population exposure to sea-level rise and the relevance for migration, Environ. Res. Lett., 15, 123005, https://doi.org/10.1088/1748-9326/abb398, 2020.

Melet, A., ~~Meyssignac, B., Almar, R., and Le Cozannet, G.: Under-estimated wave contribution to coastal sea-level rise, Nature Clim Change, 8, 234–239, https://doi.org/10.1038/s41558-018-0088-y, 2018.~~

~~Melet, A.,~~ Almar, R., Hemer, M., Cozannet, G. L., Meyssignac, B., and Ruggiero, P.: Contribution of Wave Setup to Projected Coastal Sea Level Changes, Journal of Geophysical Research: Oceans, 125, e2020JC016078, https://doi.org/10.1029/2020JC016078, 2020a.

Melet, A., Teatini, P., Le Cozannet, G., Jamet, C., Conversi, A., Benveniste, J., and Almar, R.: Earth Observations for Monitoring Marine Coastal Hazards and Their Drivers, Surv Geophys, 41, 1489–1534, https://doi.org/10.1007/s10712-020-09594-5, 2020b.

Mentaschi, L., Vousdoukas, M., Voukouvalas, E., Sartini, L., Feyen, L., Besio, G., and Alfieri, L.: Non-stationary Extreme Value Analysis: a simplified approach for Earth science applications, Global hydrology/Mathematical applications, https://doi.org/10.5194/hess-2016-65, 2016.

Meucci, A., Young, I. R., Hemer, M., Kirezci, E., and Ranasinghe, R.: Projected 21st century changes in extreme wind-wave events, Science Advances, https://doi.org/10.1126/sciadv.aaz7295, 2020.

Morim, J., Hemer, M., Cartwright, N., Strauss, D., and Andutta, F.: On the concordance of 21st century wind-wave climate projections, Global and Planetary Change, 167, 160–171, https://doi.org/10.1016/j.gloplacha.2018.05.005, 2018.

Morim, J., Hemer, M., Wang, X. L., Cartwright, N., Trenham, C., Semedo, A., Young, I., Bricheno, L., Camus, P., Casas-Prat, M., Erikson, L., Mentaschi, L., Mori, N., Shimura, T., Timmermans, B., Aarnes, O., Breivik, Ø., Behrens, A., Dobrynin, M., Menendez, M., Staneva, J., Wehner, M., Wolf, J., Kamranzad, B., Webb, A., Stopa, J., and Andutta, F.: Robustness and uncertainties in global multivariate wind-wave climate projections, Nat. Clim. Chang., 9, 711–718, https://doi.org/10.1038/s41558-019-0542-5, 2019.

Morim, J., Vitousek, S., Hemer, M., Reguero, B., Erikson, L., Casas-Prat, M., Wang, X. L., Semedo, A., Mori, N., Shimura, T., Mentaschi, L., and Timmermans, B.: Global-scale changes to extreme ocean wave events due to anthropogenic warming, Environ. Res. Lett., 16, 074056, https://doi.org/10.1088/1748-9326/ac1013, 2021.

Morim, J., Wahl, T., Vitousek, S., Santamaria-Aguilar, S., Young, I., and Hemer, M.: Understanding uncertainties in contemporary and future extreme wave events for broad-scale impact and adaptation planning, Science Advances, 9, eade3170, https://doi.org/10.1126/sciadv.ade3170, 2023.

Neumann, B., Vafeidis, A. T., Zimmermann, J., and Nicholls, R. J.: Future Coastal Population Growth and Exposure to Sea-Level Rise and Coastal Flooding - A Global Assessment, PLOS ONE, 10, e0118571, https://doi.org/10.1371/journal.pone.0118571, 2015.

O'Dea, E., Bell, M. J., Coward, A., and Holt, J.: Implementation and assessment of a flux limiter based wetting and drying scheme in NEMO, Ocean Modelling, 155, 101708, https://doi.org/10.1016/j.ocemod.2020.101708, 2020.

O'Neill, B. C., Tebaldi, C., van Vuuren, D. P., Eyring, V., Friedlingstein, P., Hurtt, G., Knutti, R., Kriegler, E., Lamarque, J.-F., Lowe, J., Meehl, G. A., Moss, R., Riahi, K., and Sanderson, B. M.: The Scenario Model Intercomparison Project (ScenarioMIP) for CMIP6, Geoscientific Model Development, 9, 3461–3482, https://doi.org/10.5194/gmd-9-3461-2016, 2016.

Pickering, M. D., Horsburgh, K. J., Blundell, J. R., Hirschi, J. J.-M., Nicholls, R. J., Verlaan, M., and Wells, N. C.: The impact of future sea-level rise on the global tides, Continental Shelf Research, 142, 50–68, https://doi.org/10.1016/j.csr.2017.02.004, 2017.

~~Pinault, J., Morichon, D., Delpey, M., and Roeber, V.: Field observations and numerical modeling of swash motions at an engineered embayed beach under moderate to energetic conditions, Estuarine, Coastal and Shelf Science, 108143, https://doi.org/10.1016/j.ecss.2022.108143, 2022.~~

Ranasinghe, R.: Assessing climate change impacts on open sandy coasts: A review, Earth-Science Reviews, 160, 320–332, https://doi.org/10.1016/j.earscirev.2016.07.011, 2016.

~~Roelvink, D., Reniers, A., van Dongeren, A., van Thiel de Vries, J., McCall, R., and Lescinski, J.: Modelling storm impacts on beaches, dunes and barrier islands, Coastal Engineering, 56, 1133–1152, https://doi.org/10.1016/j.coastaleng.2009.08.006, 2009.~~

Saint-Martin, D., Geoffroy, O., Voldoire, A., Cattiaux, J., Brient, F., Chauvin, F., Chevallier, M., Colin, J., Decharme, B., Delire, C., Douville, H., Guérémy, J.-F. -f, Joetzjer, E., Ribes, A., Roehrig, R., Terray, L., and Valcke, S.: Tracking Changes in Climate Sensitivity in CNRM Climate Models, Journal of Advances in Modeling Earth Systems, 13, https://doi.org/10.1029/2020ms002190, 2021.

~~Serafin, K. A., Ruggiero, P., and Stockdon, H. F.: The relative contribution of waves, tides, and nontidal residuals to extreme total water levels on U.S. West Coast sandy beaches, Geophysical Research Letters, 44, 1839–1847, https://doi.org/10.1002/2016GL071020, 2017.~~

Staneva, J., Grayek, S., Behrens, A., and Günther, H.: GCOAST: Skill assessments of coupling wave and circulation models (NEMO-WAM), J. Phys.: Conf. Ser., 1730, 012071, https://doi.org/10.1088/1742-6596/1730/1/012071, 2021.

~~Stockdon, H. F., Holman, R. A., Howd, P. A., and Sallenger, A. H.: Empirical parameterization of setup, swash, and runup, Coastal Engineering, 53, 573–588, https://doi.org/10.1016/j.coastaleng.2005.12.005, 2006.~~

Stokes, K., Poate, T., Masselink, G., King, E., Saulter, A., and Ely, N.: Forecasting coastal overtopping at engineered and naturally defended coastlines, Coastal Engineering, 164, 103827, https://doi.org/10.1016/j.coastaleng.2020.103827, 2021.

Toledano C., García San Martín L., Barrera Rodríguez E., Dalphinet A., Ghantous M., Aouf L., Lorente P., de Alfonso M., García Sotillo M.,: Quality Information Document (CMEMS-IBI-QUID-005-006), available at: https://catalogue.marine.copernicus.eu/documents/QUID/CMEMS-IBI-QUID-005-006.pdf (last access: 16 December 2022), 2021

Valiente, N. G., Masselink, G., Scott, T., Conley, D., and McCarroll, R. J.: Role of waves and tides on depth of closure and potential for headland bypassing, Marine Geology, 407, 60–75, https://doi.org/10.1016/j.margeo.2018.10.009, 2019.

Viitak, M., Maljutenko, I., Alari, V., Suursaar, Ü., Rikka, S., and Lagemaa, P.: The impact of surface currents and sea level on the wave field evolution during St. Jude storm in the eastern Baltic Sea, Oceanologia, 58, 176–186, https://doi.org/10.1016/j.oceano.2016.01.004, 2016.

Voldoire, A., Saint-Martin, D., Sénési, S., Decharme, B., Alias, A., Chevallier, M., Colin, J., Guérémy, J.-F., Michou, M., Moine, M.-P., Nabat, P., Roehrig, R., Mélia, D. S. y, Séférian, R., Valcke, S., Beau, I., Belamari, S., Berthet, S., Cassou, C., Cattiaux, J., Deshayes, J., Douville, H., Ethé, C., Franchistéguy, L., Geoffroy, O., Lévy, C., Madec, G., Meurdesoif, Y., Msadek, R., Ribes, A., Sanchez-Gomez, E., Terray, L., and Waldman, R.: Evaluation of CMIP6 DECK Experiments With CNRM-CM6-1, Journal of Advances in Modeling Earth Systems, 11, 2177–2213, https://doi.org/10.1029/2019MS001683, 2019.

~~Vos, K., Harley, M. D., Splinter, K. D., Walker, A., and Turner, I. L.: Beach Slopes From Satellite-Derived Shorelines, Geophysical Research Letters, 47, e2020GL088365, https://doi.org/10.1029/2020GL088365, 2020.~~

~~Vousdoukas, M. I., Mentaschi, L., Voukouvalas, E., Verlaan, M., Jevrejeva, S., Jackson, L. P., and Feyen, L.: Global probabilistic projections of extreme sea levels show intensification of coastal flood hazard, Nat Commun, 9, 2360, https://doi.org/10.1038/s41467-018-04692-w, 2018.~~

Wandres, M., Pattiaratchi, C., and Hemer, M. A.: Projected changes of the southwest Australian wave climate under two atmospheric greenhouse gas concentration pathways, Ocean Modelling, 117, 70–87, https://doi.org/10.1016/j.ocemod.2017.08.002, 2017.

Wehde H., Schuckmann K. V., Pouliquen S., Grouazel A., Bartolome T., Tintore J., De Alfonso Alonso-Munoyerro M., Carval T., Racapé V. and the INSTAC team: Quality Information Document (CMEMS-INS-QUID-013-030-036), available at: https://catalogue.marine.copernicus.eu/documents/QUID/CMEMS-INS-QUID-013-030-036.pdf (last access: 16 December 2022), 2021

Wolff, C., Nikoletopoulos, T., Hinkel, J., and Vafeidis, A. T.: Future urban development exacerbates coastal exposure in the Mediterranean, Sci Rep, 10, 14420, https://doi.org/10.1038/s41598-020-70928-9, 2020.

~~Zijlema, M., Stelling, G., and Smit, P.: SWASH: An operational public domain code for simulating wave fields and rapidly varied flows in coastal waters, Coastal Engineering, 58, 992–1012, https://doi.org/10.1016/j.coastaleng.2011.05.015, 2011.~~

Mis en forme : Couleur de police : Automatique